

2-p (mix)

X-480-71-404
PREPRINT

NASA TM X-66232

IMPROVED ITOS ATTITUDE CONTROL SYSTEM WITH HALL GENERATOR BRUSHLESS MOTOR AND EARTH-SPLITTING TECHNIQUE

WILLIAM M. PEACOCK

AUGUST 1971

(NASA-TM-X-66232) IMPROVED ITOS ATTITUDE CONTROL SYSTEM WITH HALL GENERATOR BRUSHLESS MOTOR AND EARTH-SPLITTING TECHNIQUE (NASA) 48 p HC \$4.50 CSCL 22B 48 p
N73-23858
G3/31 02981
Unclas



— GODDARD SPACE FLIGHT CENTER —
GREENBELT, MARYLAND

IMPROVED ITOS ATTITUDE CONTROL SYSTEM
WITH HALL GENERATOR BRUSHLESS MOTOR AND
EARTH-SPLITTING TECHNIQUE

William M. Peacock

August 1971

Goddard Space Flight Center
Greenbelt, Maryland

PRECEDING PAGE BLANK NOT FILMED

CONTENTS

	<u>Page</u>
ABSTRACT	v
INTRODUCTION	1
HALL EFFECT BRUSHLESS DC TORQUE MOTOR	3
MAGNETIC-PICKUP (MPU) ENCODER	9
BRUSHLESS MOTOR-DRIVE ELECTRONICS IN PLACE OF POWER AMPLIFIER	9
NARROWBAND CO ₂ SENSORS IN PLACE OF WIDEBAND SENSORS. .	11
SPLIT-HORIZON TECHNIQUE FOR EARTH REFERENCE INSTEAD OF SINGLE HORIZON DETECTION	11
CONCLUSIONS	14
REFERENCES	16

ILLUSTRATIONS

<u>Figure</u>		<u>Page</u>
1	Comparison of ITOS-A-C and ITOS-D	17
2	Dynamics-Control System Block Diagram	18
3	Dynamics-Control System Component Locations on Spacecraft .	19
4	Sequence of Events - Attitude Acquisition Showing Dynamics- Control System Element Locations on the Satellite	21
5	ITOS-D Stability Plot-Solar Panels Closed and Open	23
6	Hall Effect Brushless DC Torque Motor - Rotor and Stator . . .	24
7	Hall Effect Brushless DC Torque Motor Showing Installation of Hall Elements	25
8	Hall Effect Brushless DC Torque Motor Showing Location of Hall Elements on the Stator	26
9	Typical Speed-Torque Curve of the Hall Effect Brushless DC Torque Motor	27

Preceding page blank

ILLUSTRATIONS--(continued)

<u>Figure</u>		<u>Page</u>
10	Hall Generator	28
11	Momentum Wheel Assembly (MWA), Cross Sectional View . . .	28
12	Attitude-Sensor Configuration	29
13	Closed-Loop Pitch-Error Correction	29
14	Pitch Index Pulse Circuit	30
15	Magnetic Pickup (MPU)	30
16	Magnetic Pickup (MPU) Test Configuration Schematic	31
17	Pitch Index Pulse and Horizon-Splitting Pulse Definition	32
18	ITOS Brushless Motor Power Amplifier and Logic Drive Block Diagram	33
19	Horizon Sensor Tee Plate	34
20	Horizon Sensor, Amplifier and Threshold Circuits	35
21	Blanking Circuit	36
22	Earth Splitting	37
23	Earth Splitting Circuit	38
24	MWA Motor Housing Assembly	39
25	MWA Bearing View	40
26	MWA Oil Reservoir View	41
27	MWA Exploded View -- M1 End	42
28	MWA Exploded View -- M2 End	43
29	MWA End Cap Cutaway	44

TABLES

<u>Table</u>		<u>Page</u>
1	Mechanical Characteristics	4
2	Electrical Characteristics	5
3	Maximum Ratings (25°C unless otherwise noted)	5
4	Power Age Requirements (at 25°C ambient temperature)	7
5	Motor Vibration History	8
6	Motor Thermal Vacuum Test History	10

IMPROVED ITOS ATTITUDE CONTROL SYSTEM WITH HALL GENERATOR BRUSHLESS MOTOR AND EARTH-SPLITTING TECHNIQUE

William M. Peacock
TOS Project

ABSTRACT

The National Aeronautics and Space Administration (NASA), Goddard Space Flight Center (GSFC) will soon launch an ITOS with an improved attitude control system. A Hall generator brushless dc torque motor will replace the brush dc torque motor on ITOS-I and ITOS-A (NOAA-1).^{*} The four attitude horizon sensors will be replaced with two CO₂ sensors for better horizon definition. An earth horizon splitting technique will be used to keep the earth facing side of the satellite toward earth even if the desired circular orbit is not achieved. The external appearance of the pitch control subsystem differs from TIROS-M (ITOS 1)^{**} and ITOS-A (NOAA-1) in that two instead of one pitch control electronics (PCE) boxes are used. Two instead of four horizon sensors will be used and one instead of two mirrors will be used for sensor scanning. The PCE boxes are redundant and will contain the additional electronic circuitry for earth splitting and the brushless motor electronics. The brushless motor will eliminate the requirement for brushes, strain gages and the telemetry for the brush wear. A single rotating flywheel, supported by a single bearing provides the gyroscopic stability and the required momentum interchange to keep one side of the satellite facing the earth. Magnetic torquing against the earth's magnetic field eliminates the requirement for expendable propellants which would limit satellite life in orbit.

^{*}ITOS-A was designated NOAA-1 after launch.

^{**}TIROS-M was designated ITOS-1 after launch.

IMPROVED ITOS ATTITUDE CONTROL SYSTEM WITH HALL GENERATOR BRUSHLESS MOTOR AND EARTH-SPLITTING TECHNIQUE

INTRODUCTION

The improved attitude control system is scheduled to be first launched on ITOS-D, possibly ITOS-B or ITOS-C, if the brushless motor is ready in time for ITOS-B or C. The ITOS-B* and ITOS-C satellites will be identical to ITOS-1 and NOAA-1 except for some modifications to existing subsystems. The ITOS-D will employ sounders and radiometers in lieu of APT and AVCS cameras. Figure 1 compares the earth-facing side of ITOS-1, NOAA-1, ITOS-B, and ITOS-C with the radiometer-carrying ITOS-D that will continue to provide day and night weather coverage of the entire earth and its cloudcover. ITOS-D sensors will consist of the presently used ITOS-1/NOAA-1, scanning radiometers (SR's), and in lieu of cameras very high-resolution radiometers (VHRR's) and vertical temperature profile radiometers (VTPR's). The ITOS-D will, like previous ITOS's, measure the earth's proton and electron environment; however, it will not carry the flat-plate radiometer (FPR), which measures the amount of heat radiated into space by the earth.

ITOS-D will weigh approximately 740 pounds, as opposed to 682 pounds for previous ITOS's. The improved Delta launch vehicle with a new guidance system will place ITOS-D in the required orbit, which will have the same nominal orbital elements as for ITOS-1. The ITOS-1 orbital elements are listed below.

Semimajor axis	7840.40 km
Eccentricity	0.00023
Inclination	101.729 degrees
Mean anomaly	291.047 degrees
Argument of perigee	68.262 degrees
Motion minus	1.9182 degrees per day
Right ascension of ascending node	339.615 degrees
Motion plus	0.9842 degrees per day
Anomalistic period	115.15023 minutes
Motion plus	0.0 minutes per day
Height of perigee	1460.43 km
Height of apogee	1464.04 km
Velocity at perigee	25675 km per hour
Velocity at apogee	25663 km per hour
Geocentric latitude of perigee	65.431 degrees

* ITOS-B was launched Oct. 21, 1971 but did not go into orbit due to a booster failure. ITOS-C will be launched early in 1972 with the same brushless motor pitch-control as ITOS-B.

Figure 2 is a block diagram of the dynamics-control system for ITOS-D with asterisks (*) in the blocks that differ from ITOS-1 dynamic system components.

Figure 3 shows the locations of the dynamics-control system components on the spacecraft, as well as the half-cone look angle of the two CO₂ horizon sensors and the spacecraft-axis designations, which are the same as for ITOS-1. For design characteristics of the nutation dampers, momentum-control coils (MCC), quarter-orbit magnetic-attitude control (QOMAC) coil, magnetic-bias control (MBC) coil and switch and the digital solar-aspect sensor (DSAS), see Goddard Space Flight Center document X-481-71-108, Attitude Control Performance of the Improved Television Infrared Observation Satellite (ITOS-1), March 1971.¹

The gyroscopic stability and the principle of magnetic interaction torques have been proved successful on previous ITOS and the same stability and principles apply to ITOS-D. Figure 4 shows the sequence of events from liftoff to mission-mode acquisition, and Figure 5 is a stability plot of the satellite after separation from the Delta, showing the moments-of-inertia of the satellite axes with the solar panels open and closed, as well as the flywheel moment-of-inertia and weight of the satellite. The dotted lines in Figure 5 reveal that, if the Delta spins the satellite about its pitch axis at approximately 2.8 rpm, when the wheel reaches 115 rpm as a function of the separation switches, the satellite body rate will be about 0.7 rpm. At a wheel speed of 150 rpm, the satellite body momentum will be essentially transferred to the wheel and closed pitch-loop operation may be commanded to place the satellite in mission-mode operation. The MCC's may be used as on ITOS-1 and NOAA-1 to maintain system momentum and the desired wheel speed.

Major improvements to the attitude control of ITOS are:

- Hall effect brushless dc torque motor in place of a brush dc torque motor
- Magnetic pickup encoder for spacecraft pitch index reference in place of a variable reluctance encoder
- Brushless motor drive electronics in place of power amplifier
- Narrowband (CO₂) sensors in place of wideband sensors
- Split-horizon technique for earth pitch reference instead of single horizon detection

HALL EFFECT BRUSHLESS DC TORQUE MOTOR

The brushless dc torque motor consists of two components: a 24-pole Alnico 9 permanent-magnet rotor with its shaft mount, and a wound stator including two encoding elements (Hall generators), secured to the stator 90 electrical and 7.5 mechanical degrees apart. The motor stator has 4 windings consisting of 2 bifilar pairs. It is a pancake design which exhibits high torque-to-inertia ratio, fast response, high torque linearity, and reliability.

Figure 6 is a photograph of the rotor and stator, and Figure 7 shows the stator with Hall elements installed.

In a brush motor, proper alignment of the armature field with the stationary field poles is accomplished by proper position of the brushes which, in turn, excite the correct coils. The Hall elements in the brushless motor sense the rotor position and switch the dc voltage to the proper coil. This maintains a stator field 90 electrical degrees ahead of the rotor. The permanent magnet rotor is constantly trying to catch up to the switching stator field windings which produces motor rotation. The rotor then acts as the dc field and the stator becomes the armature. Rotor speed controls the frequency of the commutator, and true dc motor operation is obtained by using the rotor position (Hall element) sensors and solid state switches.

Figure 8 shows the position of the Hall elements on the stator to be 7.5 mechanical and 90 electrical degrees apart. The elements are mounted with the active area facing the rotor. Figure 8 also shows the configuration of the magnets, winding, and Hall elements in the brushless motor. A logic waveform is shown in the lower right corner. The motor has an outside diameter of approximately 5.5 inches and an inside diameter of approximately 3.5 inches. The approximate stator and rotor weights, less housing, is 1.2 and 0.58 pounds respectively.

Figure 9 is a typical speed-torque curve for the motor. Tables 1 and 2 list the mechanical and electrical characteristics of the motor.

The motor armature windings consist of about 20 turn coils of #30 magnet wire with 48 coils per winding and 4 windings (2 bifilar pairs). The rotor assembly elements are bonded into an integral assembly. Hall elements are bonded to the inside diameter of the stator assembly and recessed 25 mils below the stator surface (Figures 7, 8, and 10).

The rotor-pole angle, 150 electrical degrees, introduces a commutation ripple of about 17 percent. Obtaining a minimum torque ripple is not a primary performance requirement; however, the stator lamination assembly is skewed one slot to minimize slot-cogging ripple. Slot-cogging torque could exceed stall torque if zero skew is used. Thin stator laminations are used to minimize

Table 1
Mechanical Characteristics

Motor Size Constants	Units	Symbol	Value
Peak torque	lb-ft	T_P	0.39
Motor constant	(lb-ft/amp)/ $\sqrt{\text{ohm}}$	K_M	80×10^{-3}
Electrical time constant	sec	τ_E	0.0032
Power input, stalled, at peak torque (25°C)	watts	P_P	24
Viscous damping coefficients:			
a. zero impedance source	lb-ft/rad/sec	F_O	0.86×10^{-2}
b. Infinite impedance source	lb-ft/rad/sec	F_1	0.7×10^{-3}
Ripple torque, average-to-peak	percent	T_R	20
Max permissible winding temperature	°C	---	105°C
Rotor moment-of-inertia (Combined rotors)	lb-ft-sec ²	J_M	0.0108
No-load speed (theoretical)	rad/sec	W	45.3
Max motor weight (Rotor and Stator)	lb	---	1.78

core losses. Life and flight qualification tests have been performed on the Hall elements, and flight qualification testing has been performed on the brushless motor.

Table 3 lists the maximum ratings of the Hall elements and Table 4 lists power-age requirements. Brushless motor electronics (BME) provides commutating of the brushless motor and a pulse-frequency input for the tachometer circuit. Electrical requirements are:

Table 2
Electrical Characteristics

Winding Constants	Units	Tolerances	Symbol	Value
DC resistance (20°C)	Ohms	±3%	R_M	24
Volts at peak torque (25°C)	Volts	Nom	V_P	24
Amps at peak torque	Amps	Rated	I_P	1.00
Torque sensitivity	lb-ft/amp	±10%	K_T	0.39
Back EMF	Volts/rad/sec	±10%	K_B	0.531
Inductance	Henries	±10%	L_M	7.8×10^{-3}

Table 3
Maximum Ratings
(25°C unless otherwise noted)

Characteristic	Symbol	Value
Operating temperature range	°C	-65 to +100
Storage temperature range	°C	-65 to +105
Maximum continuous control current, I_{cmos} (in static air, $B \leq 3$ kG.)	ma	40
Maximum continuous control current I_{cmos} (in static air, $T_{air} > 25^\circ\text{C}$)	ma	$\sqrt{\frac{120 - T}{6.4 \times 10^4}}$
Maximum power (in static air)	mw	130

<u>Parameters as Defined in MIL-STD-793-1 WP</u>	<u>Specification Limits</u>
Nominal control current, I_{cn}	20 ma
Input resistance, R_{in}	40 to 80 ohms
Output resistance, R_{out}	$2.5 \times R_{in}$ (approx)
Resistive null voltage, V_M ($B = 0$, $I_c = 20$ ma)	6 mv max
Linearity error F% (0-5 kg) when terminated with $R_{lin} < 1K$ ohm	5% max (percent of reading)
Linearity error F% (0-5 kg) when terminated with $R_{lin} > 1K$ ohm	2% max (percent of reading)
Open circuit Hall voltage, V_{HOC} ($I_c = 10$ ma, $B = 1.0$ kG.)	$12 \text{ mv} \pm 4 \text{ mv}$
Reversibility error of V_{HOC} (0-5 kg)	2% max
Temperature coefficient of V_{HOC} , mean value (-40 to +100°C)	-0.1%/°C max
Thermal resistance Hall plate to ambient, $R_{th P-A}$	0.8°C/mw approx
Hall plate to encapsulation, substrate side only, $R_{th P-E}$	0.04°C/mw approx
Noise, mv p-p	20 (typical)
Temperature dependence of V_M ($I_c = 20$ ma)	$10 \mu\text{v}/^\circ\text{C}$ max
Temperature coefficient of R_{in} and R_{out}	0.1%/°C approx
Polarity: With field direction as shown in Figure 10 and I_c entering the red lead, the positive Hall output voltage will appear at the blue lead.	

Table 4
Power Age Requirements
(at 25°C ambient temperature)

Requirement Test	Reference	Conditions	Symbol	Acceptance Criteria		
				Initial -final	Min. Limit	Max. Limit
Linearity error open circuited	MIL-STD-793-1 (WP)	0 - 5 kG. $I_c = 20\text{ma}$	$F\%$	$\pm 5\%$	---	5%
Resistive null voltage	MIL-STD-793-1 (WP)	$B = 0$ $I_c = 20\text{ma}$	V_M	50% or 500 μv whichever is greater	---	6mv
Open circuit Hall voltage	MIL-STD-793-1 (WP)	$I_c = 10\text{ma}$ $B = 1.0 \text{ kG.}$	V_{HOC}	$\pm 2\text{mv}$	8mv	16mv

The motor rotor is supported by a single four-point bearing lubricated by P-10 oil from an oil reservoir in the motor housing. The bearing and P-10 oil have been flown on the brush motors of ITOS-1 and NOAA-1, and are, therefore, considered qualified for the brushless motor. The nominal motor speed for the ITOS is 150 rpm. Figure 11 shows the MWA with brushless motor, single mirror configuration disc, and magnetic pickup. Tables 5 and 6 show motor-vibration and motor thermal-vacuum, test histories. Figure 12 shows the fixed sensors view to the single rotating mirror. The thin-film test history is as follows:

BELL INC.

5 units in life test 650 days at (3 at 25°C, 2 at 100°C)

No failures to date
No drift out of spec.

RCA

3 units immersed in P-10 oil 210 days

No failures to date
No drift out of spec.

RCA

Thermal vacuum and vibration as part of
MWA indicated prior.

Table 5
Motor Vibration History

Unit	Vibration Type	Frequency Band (cps)	Acceleration Density (g ² /cps)	Duration	Level G-rms	Level G-0- PK	Sweep Rate (one sweep per axis)
1 (ITOS)	Random Sinusoidal	20-2000 5-2000	0.2 Bulk type	4 min/axis Hall element	20	10	2 octaves/min
2	Random Sinusoidal	20-2000 20-400	0.24 Thin film	2 min/axis Hall element	21.8	13.5	2 octaves/min
3	Random	20-2000	0.13 Thin film	2 min/axis Hall element	16		
4	Random	20-2000	0.13 Thin film	2 min/axis Hall element	16		

MAGNETIC-PICKUP (MPU) ENCODER

The MPU encoder will be used on ITOS-D to provide the satellite earth-facing side reference. The MPU pulse-occurrence time is compared to the occurrence time of an earth-splitting pulse. If the two pulses occur simultaneously, there is no pitch error and the satellite earth facing side is pointing toward the center of earth. If the MPU pulse does not occur coincident with the earth-splitting pulse, then there is a pitch error, and motor current will be automatically changed by the pitch control electronics (PCE) to change wheel speed, thereby maintaining the earth-facing sensors toward the center of earth. The method of changing wheel speed shown in Figure 13 is essentially the same as that used on ITOS. The difference between the MPU for ITOS-D and that used on ITOS-1 and NOAA-1 is the method used to generate the pulse for ITOS-D and the fact that the ITOS-D is not as wheel-speed-dependent as ITOS-1 and NOAA-1. The ITOS-1 and NOAA-1 pulse was generated by a magnet rotating past a pulse-pickup coil, whereas the ITOS-D MPU pulse will be generated when a slot in a disk rotates past the MPU. The MPU for ITOS-D consists of two magneto resistors and associated electronic circuitry. The approximate wheel speed where the ITOS-D MPU is expected to drop out is 15 rpm as compared to 90 rpm for ITOS 1 and NOAA 1.

Figure 11 shows the MPU location in the momentum-wheel assembly (MWA) and Figure 14 the schematic for circuitry in the MPU. Figure 15 is a schematic of the MPU, which has not been flown by NASA but is being flight-qualified for ITOS. There is a MPU for each pitch loop and one disk is used for both MPU's. Figure 16 shows the MPU electrical test configuration and pickup configuration in the MWA. It will be helpful to review the location of the MPU in the MWA shown in Figure 11 along with Figures 14, 15, and 16. The 12 mil clearance between the MPU and disk far exceeds the 6.5 to 9.5 mil clearance of the ITOS-1, NOAA-1, magnetic pickup. The spacecraft reference or magnetic pickup or pitch index pulse (PIP) will occur at the same point in wheel rotation regardless of spacecraft attitude. When there is no pitch error, the PIP will be coincident with the horizon-sensor earth-splitting pulse and there will be no error signal to change wheel speed (see Figure 17). Figure 13 shows the feedback pitch loop action to change wheel speed when pitch errors occur.

BRUSHLESS MOTOR-DRIVE ELECTRONICS IN PLACE OF POWER AMPLIFIER

Commutation signals are derived from the field of the permanent-magnet rotor. The field is unique over the span of one pole pair but is periodic for the entire rotor (twelve cycles per revolution corresponding to twelve pole pairs). The Hall elements mounted in the stator sense the magnetic field to provide position

Table 6
Motor Thermal Vacuum Test History

Units	Speed	Temp. (°C)	Running Time (Days)	Type of Test	Hall Elements
1 ITOS	150	-15 +60	0.75 0.75	Prototype	Bulk
1 ITOS	400 rpm 85% of time 150 rpm 15% of time	- 5 +10 +25 +35	29.0 47.0 30.0 49.0	R&D	Bulk
2	150	- 5 +15 +25 +45	1.5 30.0 1.0 1.5	Design proof	Thin film
3	150	+15 - 5 +45	0.5 0.5 0.5	FAT*	Thin film
4	150	+15 - 5 +45	0.5 0.5 0.5	FAT*	Thin film

*Flight Acceptance Test (FAT)

information. Signals from the Hall elements are detected and applied to the control and commutation logic (CCL). The CCL encodes the rotor position information and directs the tach-loop signal (either forward or reverse torque) to the proper motor driver and its associated winding (Figure 18). As the motor rotates the winding energization is switched to provide commutation. The motor drivers serve the purpose of both commutation switches and power amplifiers. Two identical PCE boxes per satellite, located on the inside base plate surface near the MWA, contain all electrical functions required for two redundant pitch loops; the MWA contains the horizon sensors and associated electronics, the flywheel, one bearing, a oil reservoir, two brushless dc torque motors, one scanning-mirror assembly, two encoders, and two labyrinth seals. Figure 19 is a view of the horizon-sensor tee plate assembled into and part of the MWA. Comparison of Figures 19 and 20 shows how the fixed horizon sensors view the rotating mirror. The electronic circuitry contains a motor-winding disconnect relay for each pitch loop to prevent an electronic failure in one loop

from loading the other motor. Motor current and voltage in addition to the status of all relays will be monitored on telemetry.

NARROWBAND CO₂ SENSORS IN PLACE OF WIDEBAND SENSORS

The sensors used on ITOS-1 (NOAA-1) were sensitive in the 8- to 20-micron range. The narrowband sensors for ITOS-D and possibly ITOS-B and C are sensitive in the 14- to 16-micron range; therefore, there will be no moon interference, and signal definition for the sky-earth and earth-sky crossings will be much sharper making computer attitude determination reliable. The signal strength shall not be sufficient to generate a threshold level output for the following radiance sources:

- The sun, when the angle between the sun and the sensor axis is greater than 4 degrees
- The moon
- The spacecraft antennas

The signal threshold to peak to peak noise ratio shall be greater than 4 to 1 when the radiance difference between the sources is 3.7×10^{-4} watts/cm² steradian or greater in the 14- to 16-micron wavelength region. The field-of-view between the half-power points shall be 2.75 degrees.

In the mission mode, the sun is at an angle of approximately 45 degrees to the positive pitch axis and the horizon sensors scan through the rotating mirror, a half-cone angle of 50 degrees about the negative pitch axis. Therefore, the sensors should never see the sun. If sensors should see the sun, recovery time of the electronics after a direct view of the sun on the optical areas shall not exceed 1 second.

Figure 20, a block diagram of the horizon-sensor amplifier and threshold circuits, should be compared with Figure 2. Also, blanking circuits are incorporated to eliminate negative and positive overshoot as shown in Figure 21.

SPLIT-HORIZON TECHNIQUE FOR EARTH REFERENCE INSTEAD OF SINGLE HORIZON DETECTION

The use of CO₂ sensors has made possible an earth-splitting technique which will generate a pulse representing the center of earth as long as the attitude of

the spacecraft is such that the horizon sensors scan the earth. The earth-splitting pulsetime occurrence is compared to the time the spacecraft reference (or PIP) occurs and keeps a momentum exchange between the wheel and the spacecraft body such that the earth facing side of the satellite faces the earth even for elliptical orbits. The position error detector uses pulsewidth modulation to measure the time difference between the split horizon pulse and the PIP. An error signal is produced with constant amplitude, variable pulsewidth, and either polarity. The width of the error signal is proportional to the magnitude of the angular error and the polarity is a function of its direction.

Two counters are provided in each pitch loop. The counters are triggered by the horizon sensor threshold signals and for the first sky-earth and earth-sky transitions the counters count at the same rate. The next sky-earth threshold signal causes counter 2 to count at twice the original rate thereby generating the split horizon pulse which is delayed by one spin period as revealed in Figure 22. The counts and counter rate are also revealed in this figure. Figure 23 is a block diagram of the earth-splitting circuit. The counting cycle repeats itself as shown in Figure 22.

- Roll Attitude Determination Random Error Summary

<u>Category/Error Source</u>	<u>Angular Error (deg) (3σ - Value)</u>
a. Noise and Ground Data Processing	± 0.031
b. Flywheel Unbalance	± 0.0002
c. Bearing Free Motion	± 0.009
d. Uncompensated Angular Momentum	<u>± 0.025</u>
RSS Summation (3σ - Value)	± 0.041

- Roll Attitude Determination Bias Error Summary

<u>Category/Error Source</u>	<u>Angular Error (deg) (3σ - Value)</u>
a. Attitude Sensing	
1. Alignment Uncertainty	± 0.013
2. Altitude Uncertainty	± 0.011
3. Sensor Dynamic Error	± 0.034
4. Earth Oblateness	± 0.176
5. Horizon Variation	± 0.086
b. Dynamic Unbalance	<u>± 0.018</u>
RSS Summation (3σ - Value)	± 0.200

- Roll Pointing Error (ϕ Max) Summary

<u>Category/Error Source</u>	<u>Angular Error (deg) (3σ/Worst-Case-Values)</u>
a. Attitude Determination	
1. Random Error Contributions	$\pm 0.0545^*$
2. Flywheel Unbalance	± 0.0005
3. Bearing Free Motion	± 0.027
4. Uncompensated Angular Momentum	± 0.025
b. Cyclic External Disturbances	
1. Solar Pressure Torque	± 0.018
2. Gravity Gradient Torque	± 0.053
3. Magnetic Torque	<u>± 0.034</u>
RSS Summation (3σ - Value)	± 0.093
c. Secular External Disturbances	
1. Solar Pressure Torque	± 0.054
2. Magnetic Torque	<u>± 0.028</u>
Vector Summation (Worst Case Value)	± 0.061
d. Attitude Determination	
Bias Error Contribution	<u>± 0.200</u>
Worst Case Summation	± 0.354

*Predicated on the least squares fit of 21 samples of attitude data, derived at 30 second intervals, each characterized by a 3σ random uncertainty of ± 0.041 degree.

- Pitch Pointing Error (Op) Summary

<u>Category/Error Source</u>	<u>Angular Error (deg) (3σ - Value)</u>
a. Attitude Sensing	
1. Alignment Uncertainty	± 0.017
2. Sensor Calibration	± 0.100
3. Threshold Uncertainty	± 0.180
4. Sensor Dynamic Error	± 0.044
5. Earth's Oblateness	± 0.171
6. Horizon Variation	± 0.090
b. Servo Loop Tolerances	± 0.100
c. Momentum Variation	<u>± 0.081</u>
RSS Summation (3σ - Value)	± 0.314

- Uncompensated Angular Momentum Summary for ITOS-D Spacecraft

<u>Component</u>	<u>Uncompensated Angular Momentum (in.-lb.-sec.)</u>
a. Scanning Radiometer	0.025
b. Very High Resolution Radiometer	0.125
c. Verticle Temperature Profile Radiometer	
1. Filter Wheel and Chopper Drive	0.0625
2. Scanning Mechanism and Mirror Drive	0.0625
d. Scanning Radiometer Recorder	0.020
e. Very High Resolution Radiometer Recorder	0.020

CONCLUSIONS

The predicted performance of ITOS with the previously described pitch control subsystem in regard to pointing accuracy is ± 0.354 degree in roll and ± 0.314 degree in pitch. The contributors to these errors are listed as shown above. In addition the uncompensated angular momentum effects are also listed.

The absence of brushes will alleviate the thermal problems encountered by ITOS-1 and NOAA-1 (reference 1) in the brushless-motor pitch-control subsystem.

Although the bearing for ITOS-1 and NOAA-1, is the same as will be used on the ITOS brushless pitch-control subsystem, there is no reason to suspect bearing problems in the absence of brushes. The bearing is the Kaydon KD45XP with selected diametral clearances between 0.008 and 0.0012 inch. The angular tilt is held to 0.00045-radian maximum. Allowable load values on the bearing, based on a standard usable Brinell value, are:

Radial load	12,400 pounds
Thrust load	30,800 pounds
Moment	31,000 pound-inches

Details of the bearing appear in volume 2-VIII-78 of reference 3.

If an electronic failure in a pitch loop should apply excess current to a motor winding, the motor-heating effect, which may cause a bearing problem, can be relieved by opening the path to the particular motor by ground-station command to open relay contacts in series with the four motor windings.

Heaters provided on the MWA ensure proper oil viscosity for bearing lubrication if cold conditions in orbit require the heat.

The gymnastics and recapture performed by ITOS-1 and NOAA-1 have proved the ITOS dynamic stability to be unquestionable (see reference 1). ITOS-1 has recaptured after a wheel-stop condition for several days and the NOAA-1 has recovered after several orbits with the wheel stopped.

The dynamic-suspension test and computer analysis will be performed to ensure acquisition and mission-mode performance during the operation and switching of pitch loops and switching of all other spacecraft subsystems.

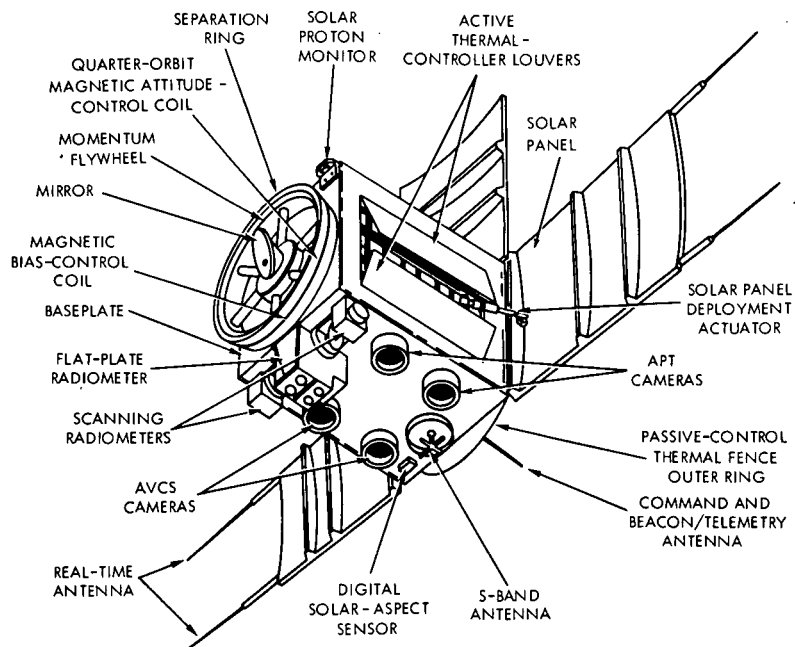
All mechanical clearances in the MWA have been verified theoretically and by tilt-testing the MWA to ensure no rubbing.

In addition, bearing-noise telemetry and bearing temperature will be monitored in orbit as a basis for the MWA heater requirement.

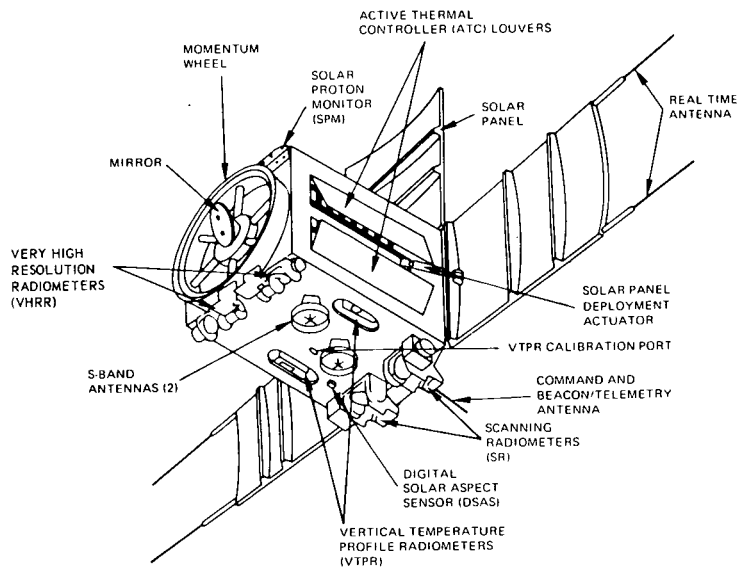
The MWA and a breakdown of its parts are identified in Figures 24, 25, 26, 27 and 28. The horizon sensor tee plate is not shown here but reference to Figures 11 and 19 along with Figures 24 through 28 will be helpful. Figure 29 shows how the magnetic pickups and disc are installed in the M-2 end of the MWA.

REFERENCES

1. GSFC Document X-481-71-108, March 1971
2. Contract NAS5-10306, Performance Specifications for ITOS-D-Dynamic Subsystems
3. Final Design Report ITOS-A, NASA Contract Number NAS5-10306
4. RCA-Major Design Review Material for ITOS Brushless Motor-Pitch Control Subsystem

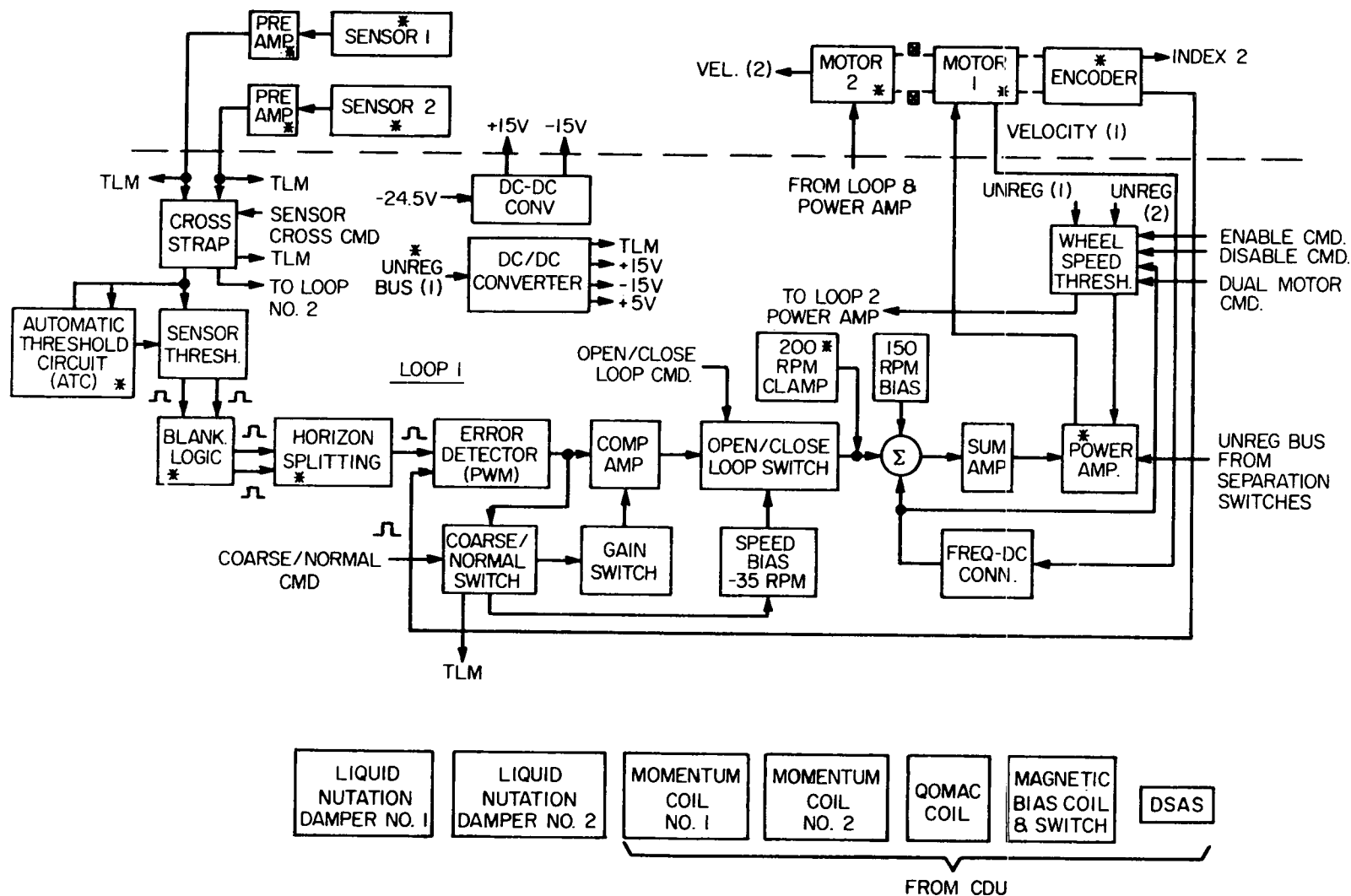


ITOS-A-C Spacecraft



ITOS-D Spacecraft

Figure 1. Comparison of ITOS-A-C and ITOS-D



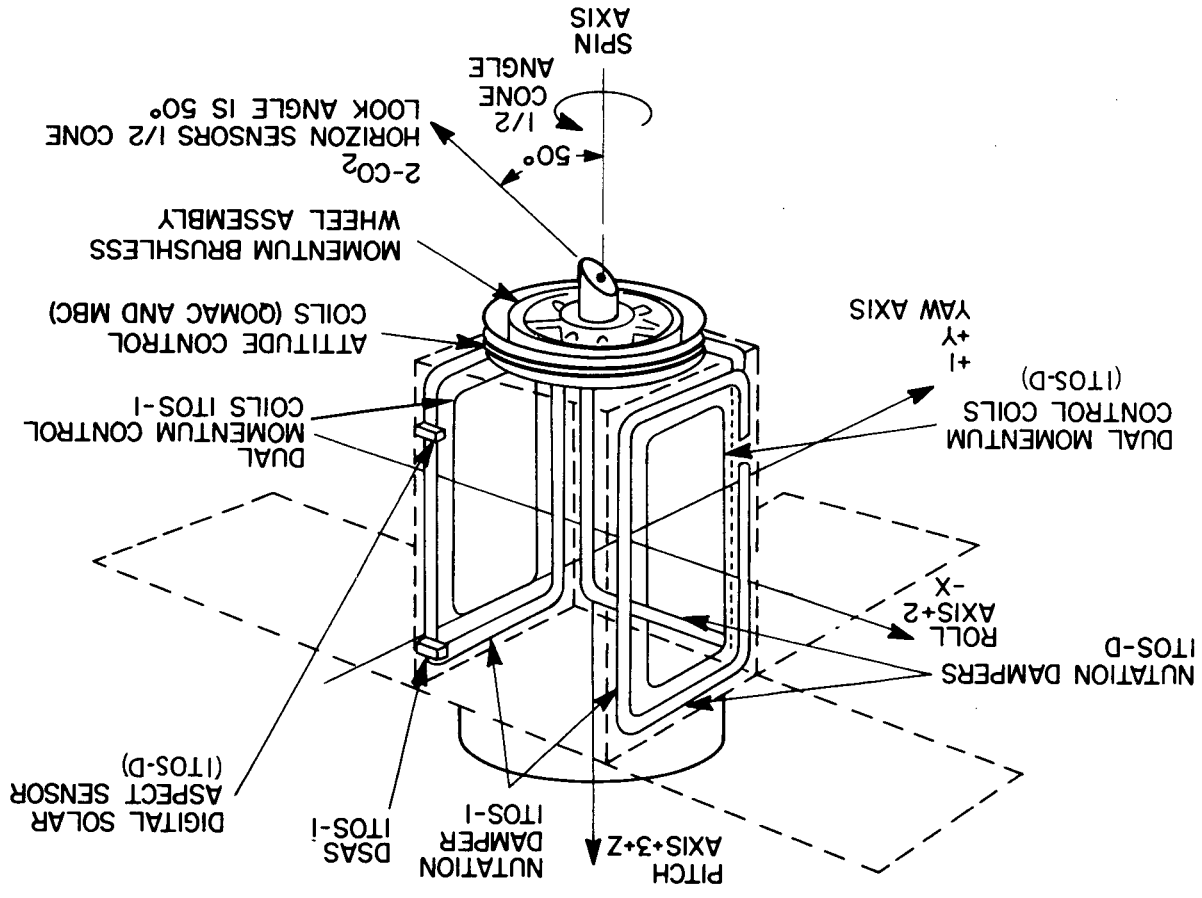
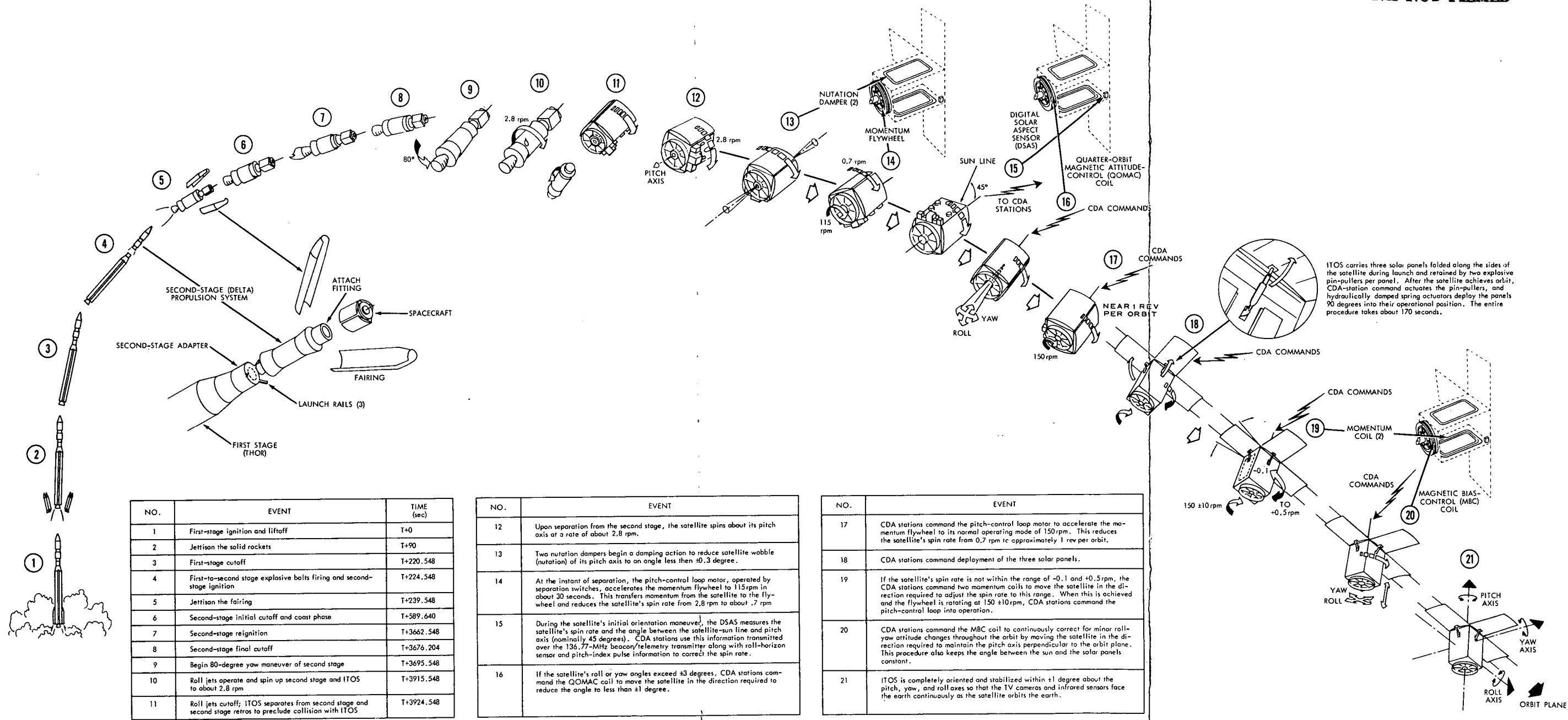


Figure 3. Dynamics-Control System Component Locations on Spacecraft

PRECEDING PAGE BLANK NOT FILMED



NOTE: Satellite Sensors and Dynamics Components shown here are for ITOS-1, NOAA1, ITOS-B and C. For ITOS-D see Figures 1 and 3.

Figure 4. Sequence of Events — Attitude Acquisition Showing Dynamics-Control System Element Locations on the Satellite

Preceding page blank

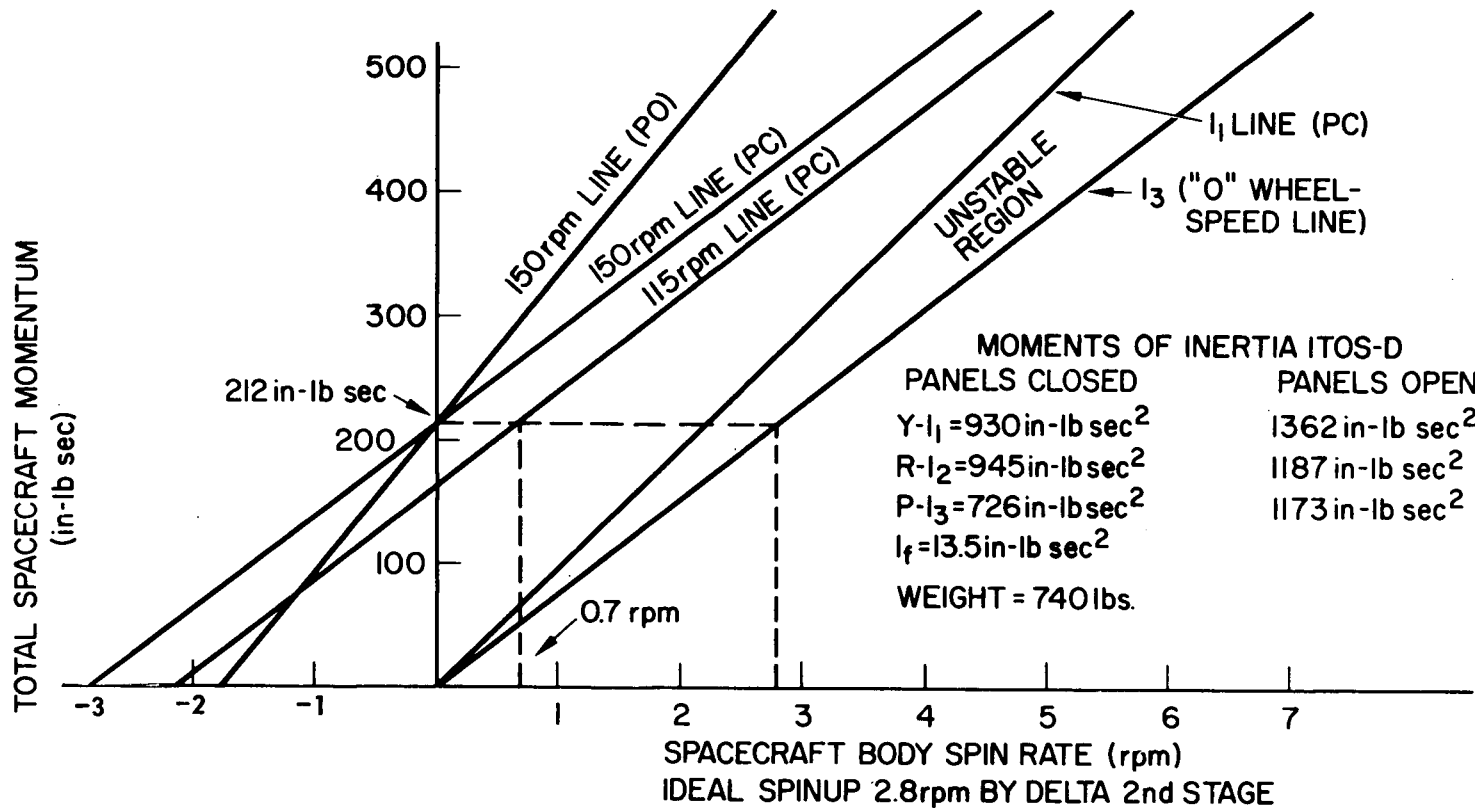


Figure 5. ITOS-D Stability Plot – Solar Panels Closed and Open

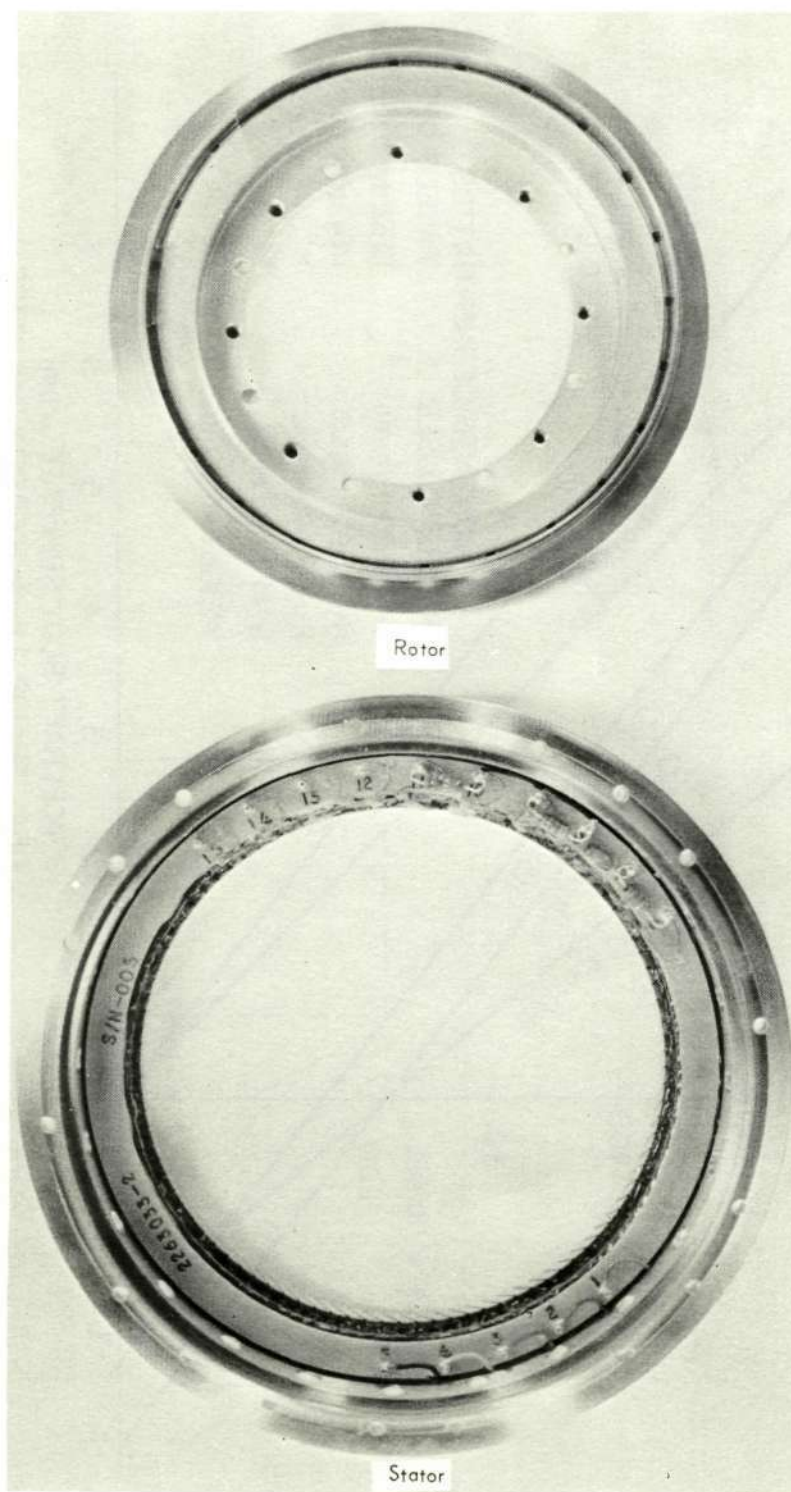
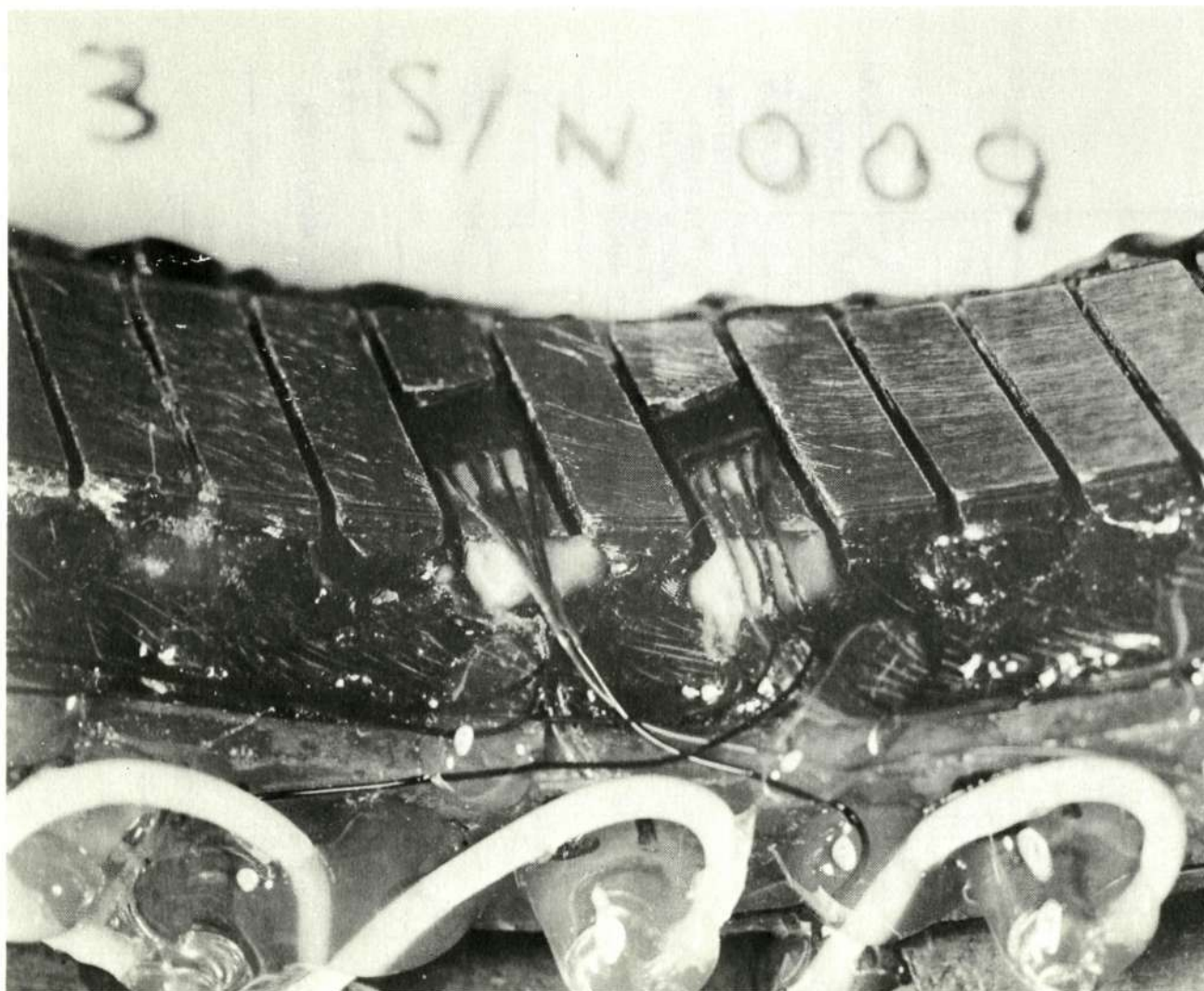


Figure 6. Hall Effect Brushless DC Torque Motor – Rotor and Stator



Reproduced from
best available copy.

Figure 7. Hall Effect Brushless DC Torque Motor Showing Installation of Hall Elements

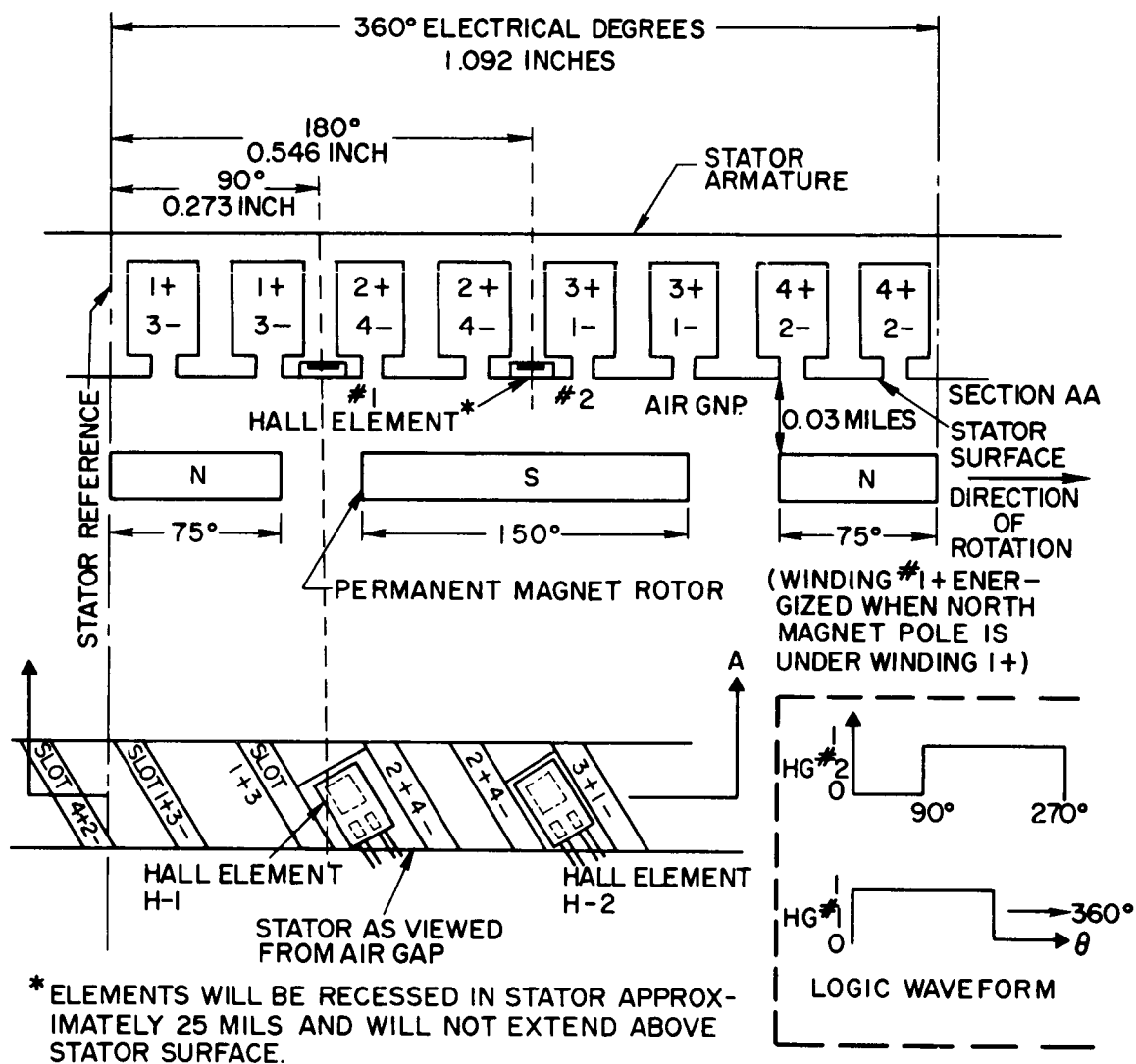


Figure 8. Hall Effect Brushless DC Torque Motor Showing Location of Hall Elements on the Stator

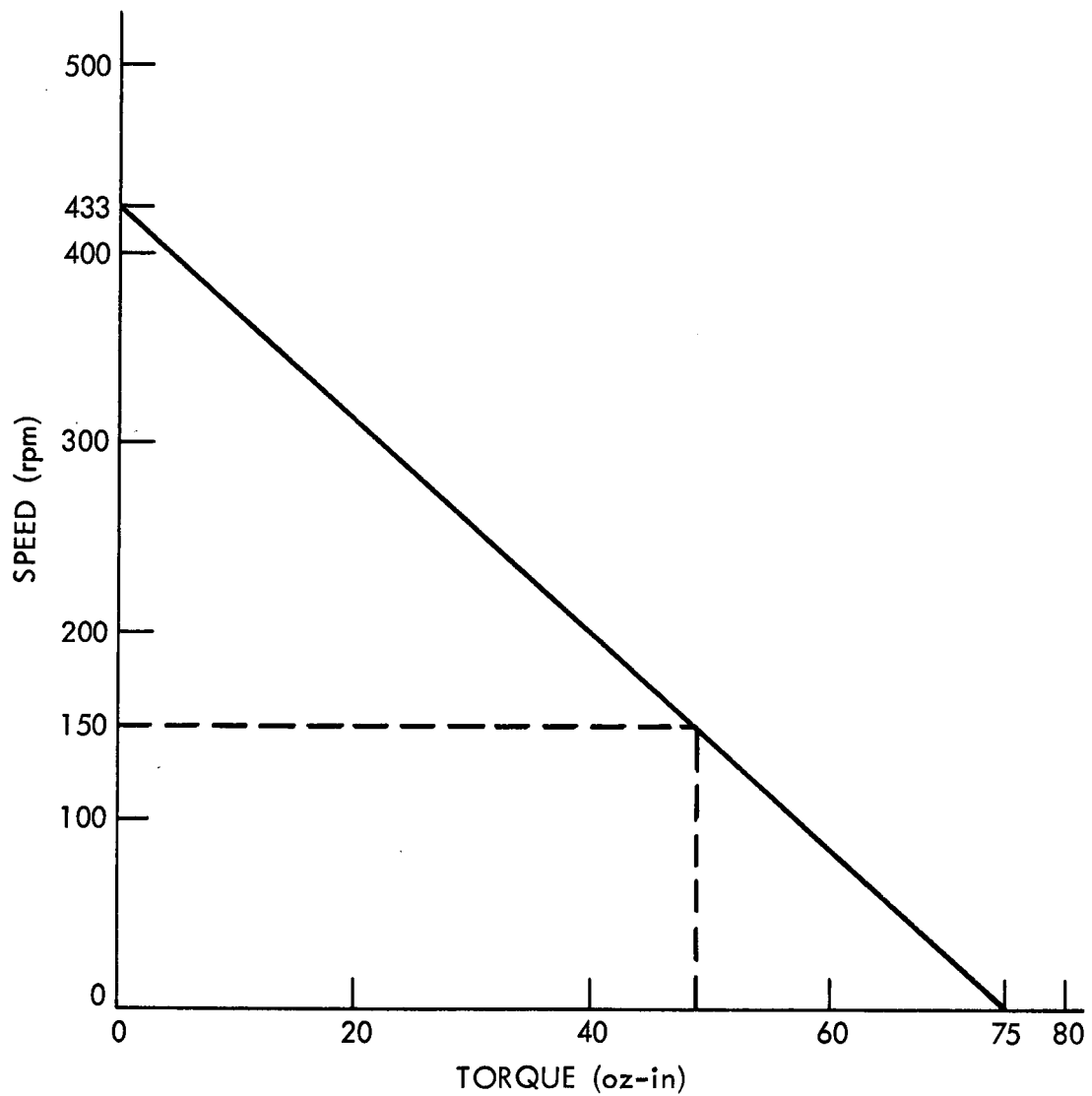


Figure 9. Typical Speed-Torque Curve of the Hall Effect
Brushless DC Torque Motor
Applied Voltage = - 24 V

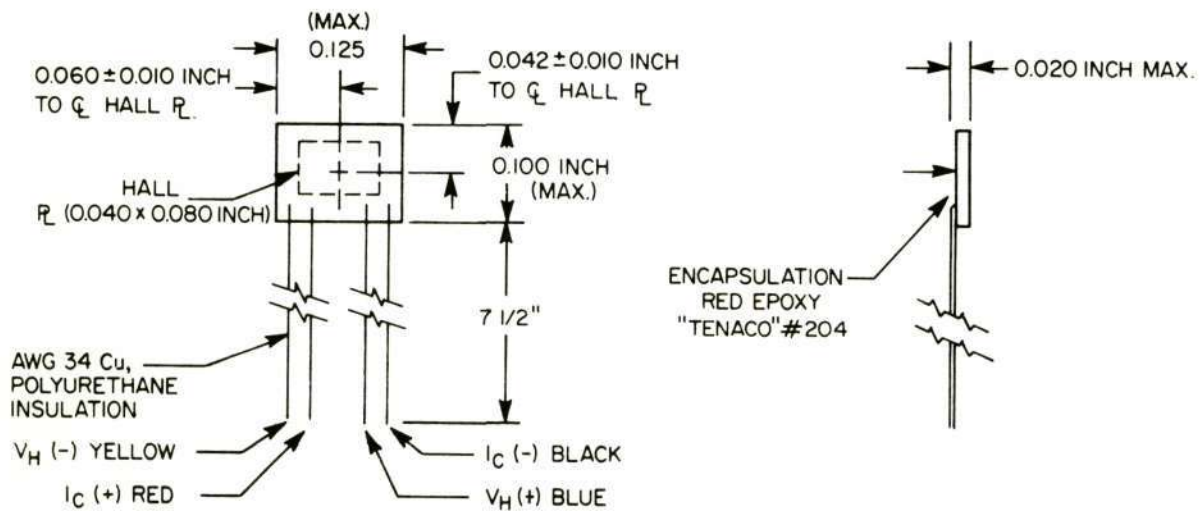


Figure 10. Hall Generator

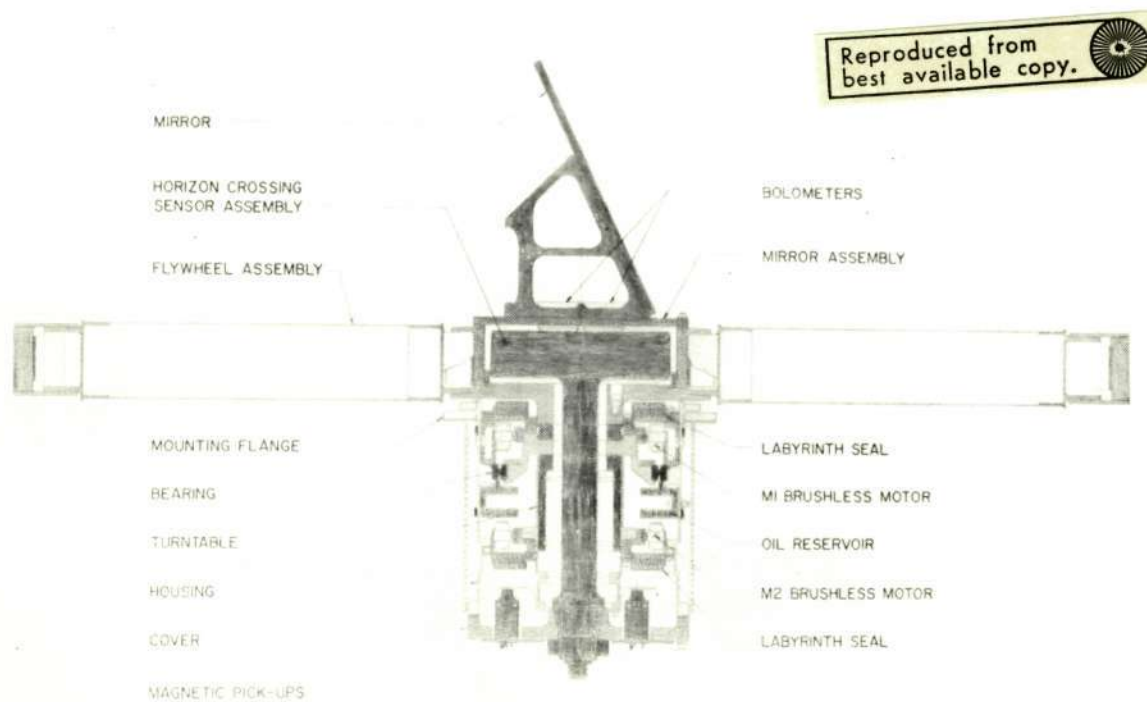


Figure 11. Momentum Wheel Assembly (MWA), Cross Sectional View

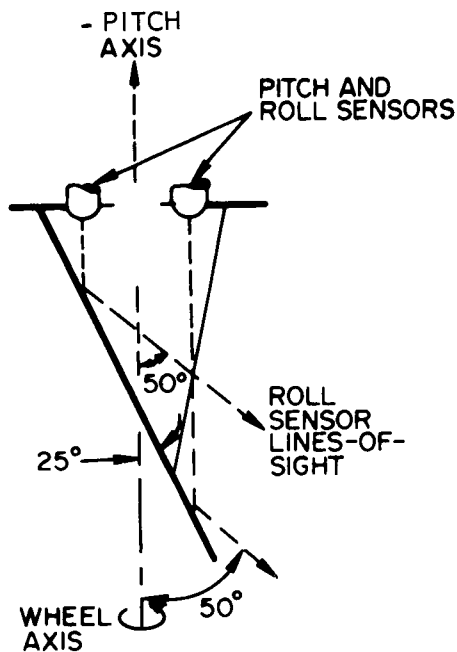


Figure 12. Attitude-Sensor Configuration

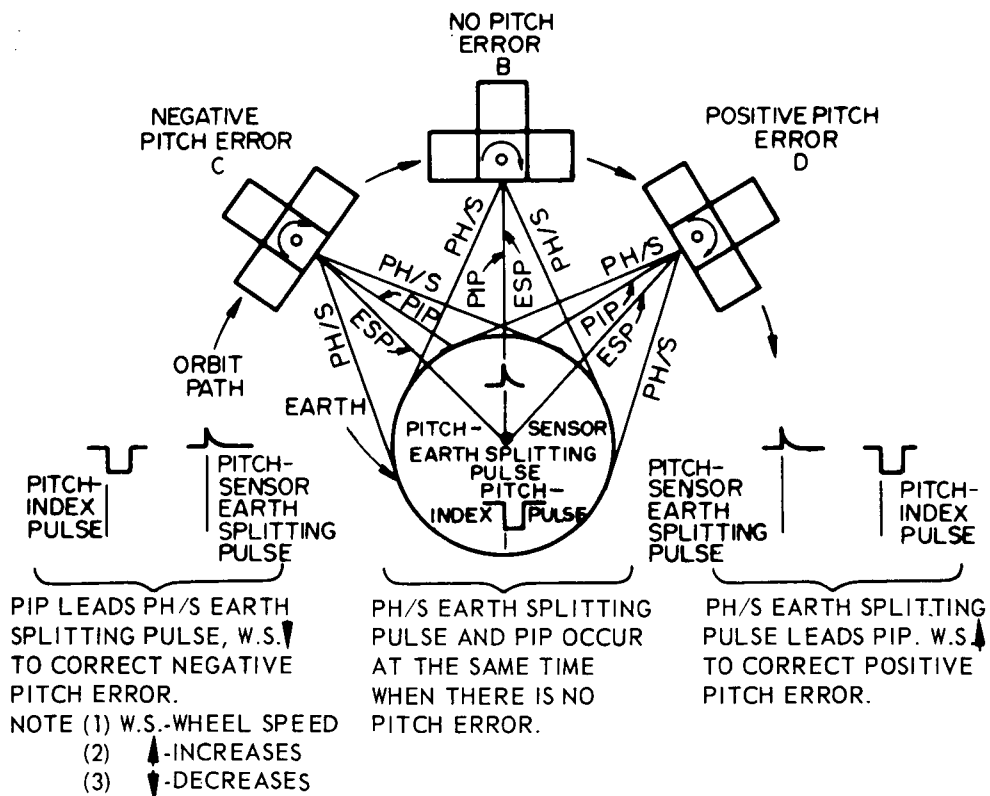


Figure 13. Closed-Loop Pitch-Error Correction

FILTER ADDED EXTERNAL TO
CIRCUIT TO PREVENT POWER
LINE NOISE FROM TRIGGERING
PULSE CIRCUIT

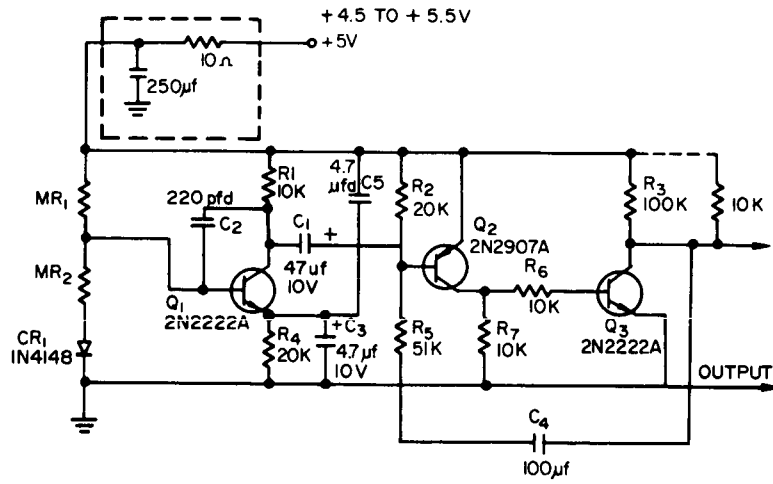


Figure 14. Pitch Index Pulse Circuit

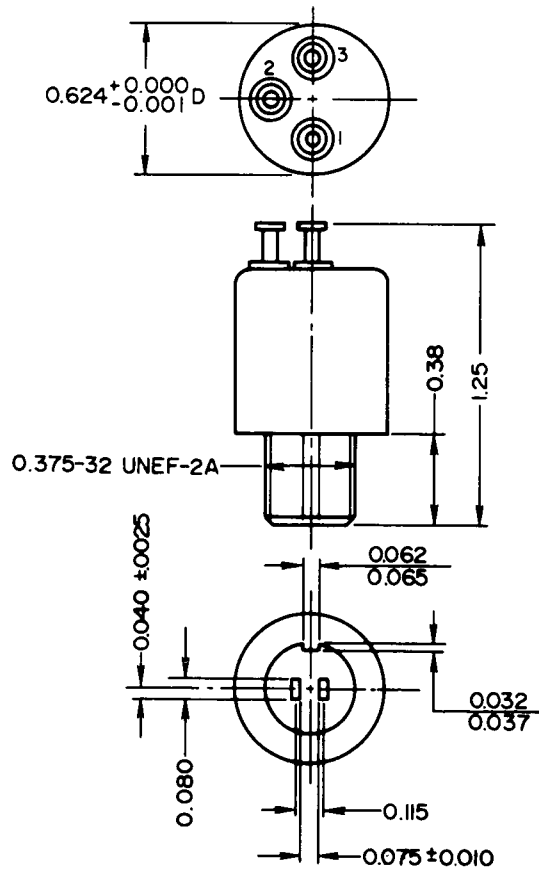


Figure 15. Magnetic Pickup (MPU)

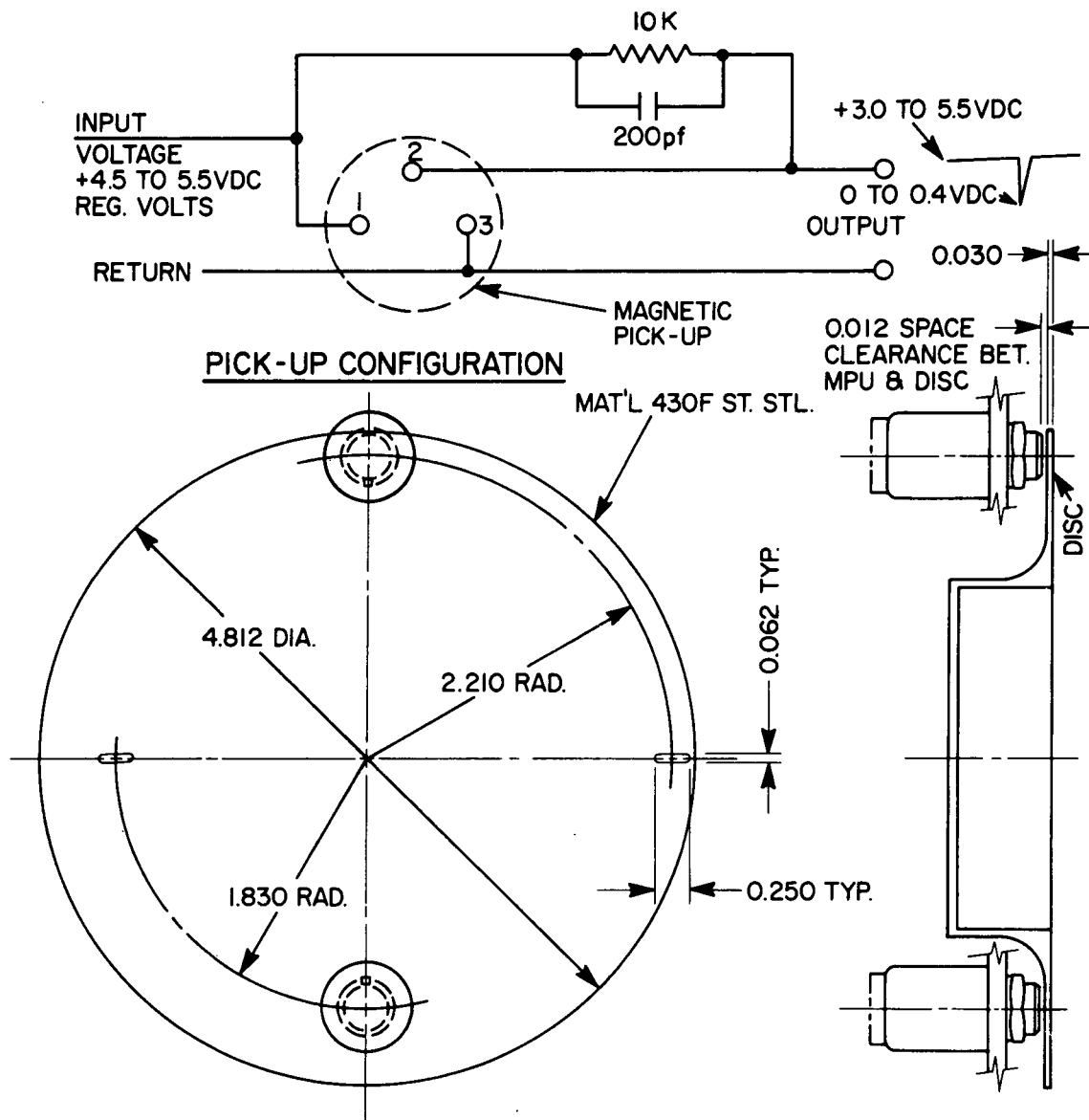


Figure 16. Magnetic Pickup (MPU) Test Configuration Schematic

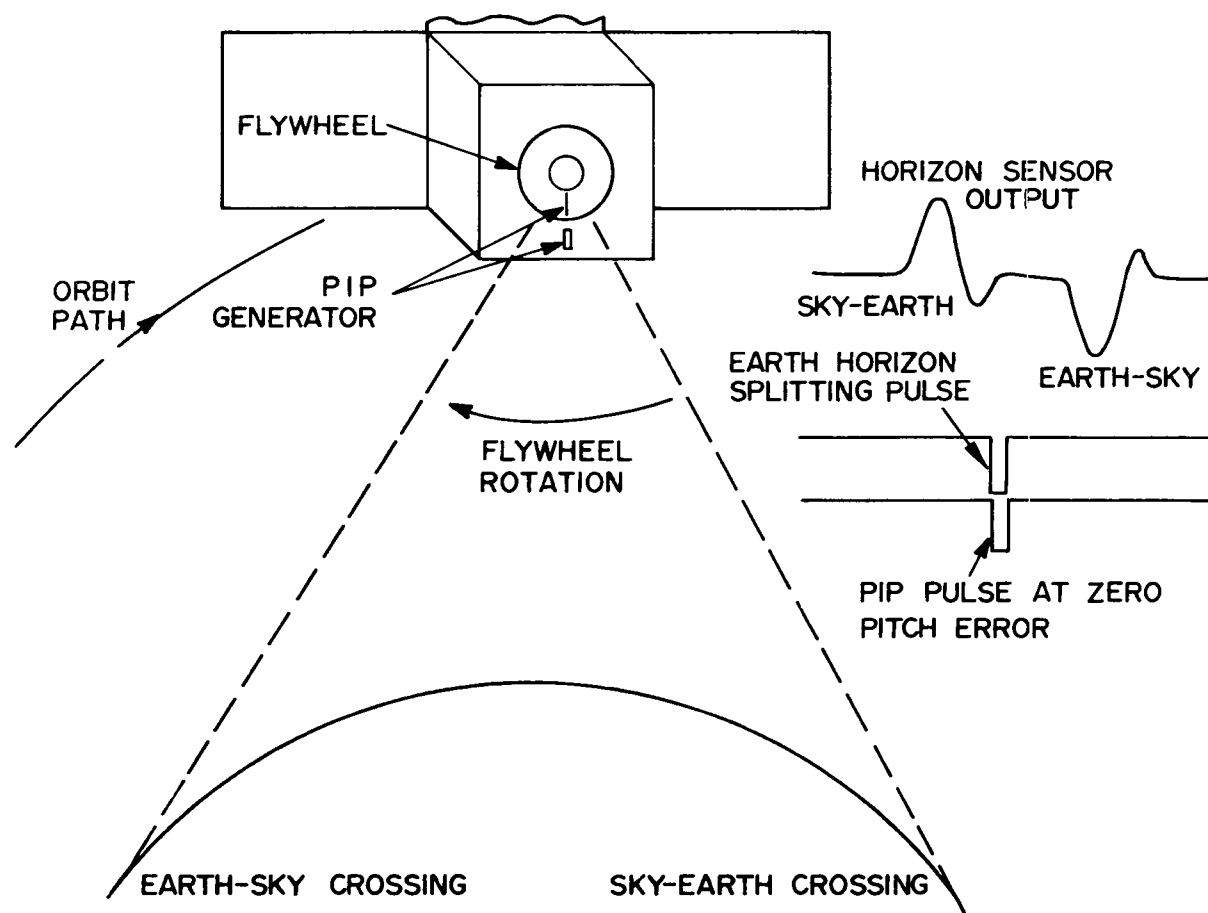


Figure 17. Pitch Index Pulse and Horizon - Splitting Pulse Definition

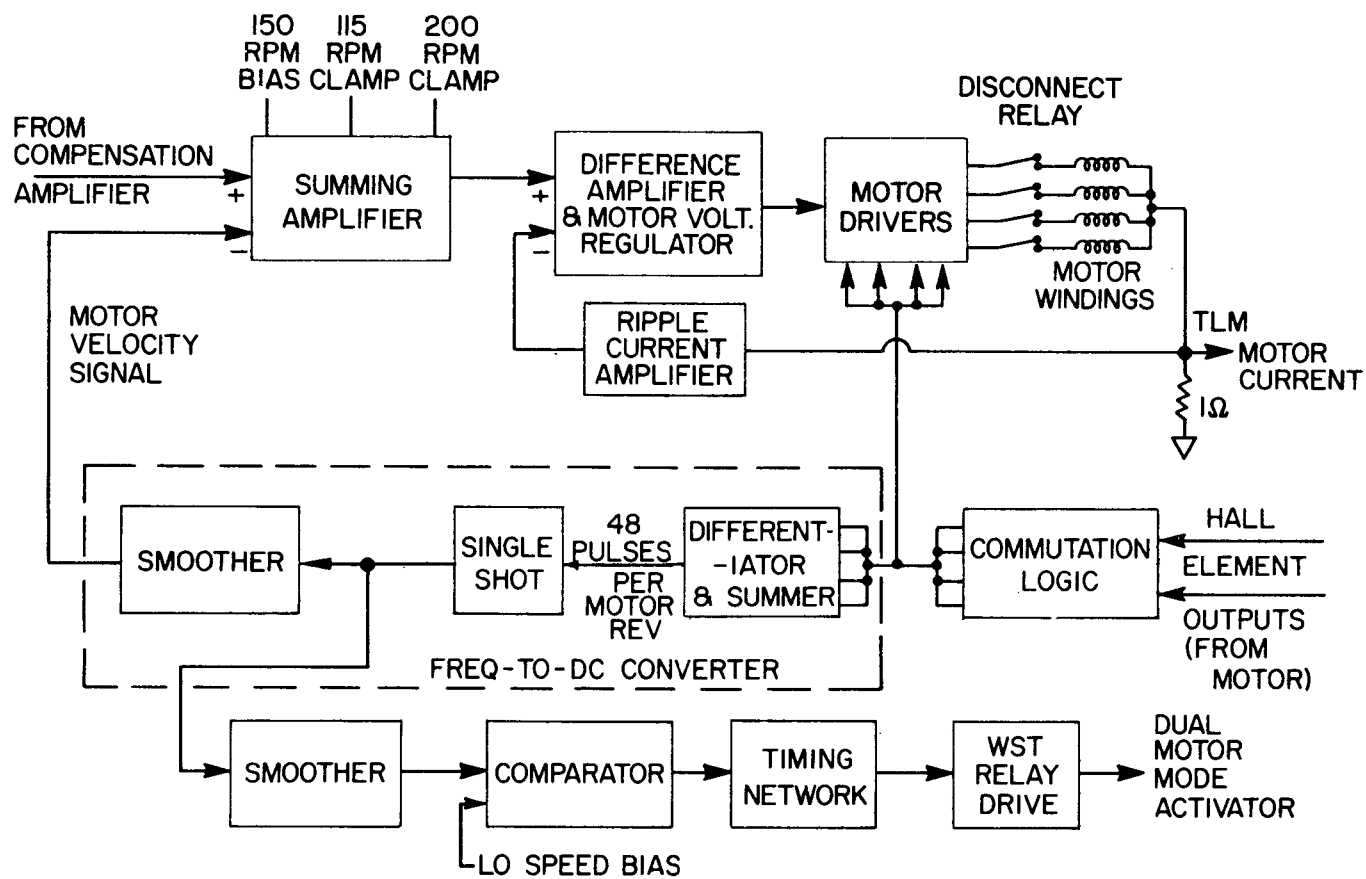


Figure 18. ITOS Brushless Motor Power Amplifier and Logic Drive Block Diagram

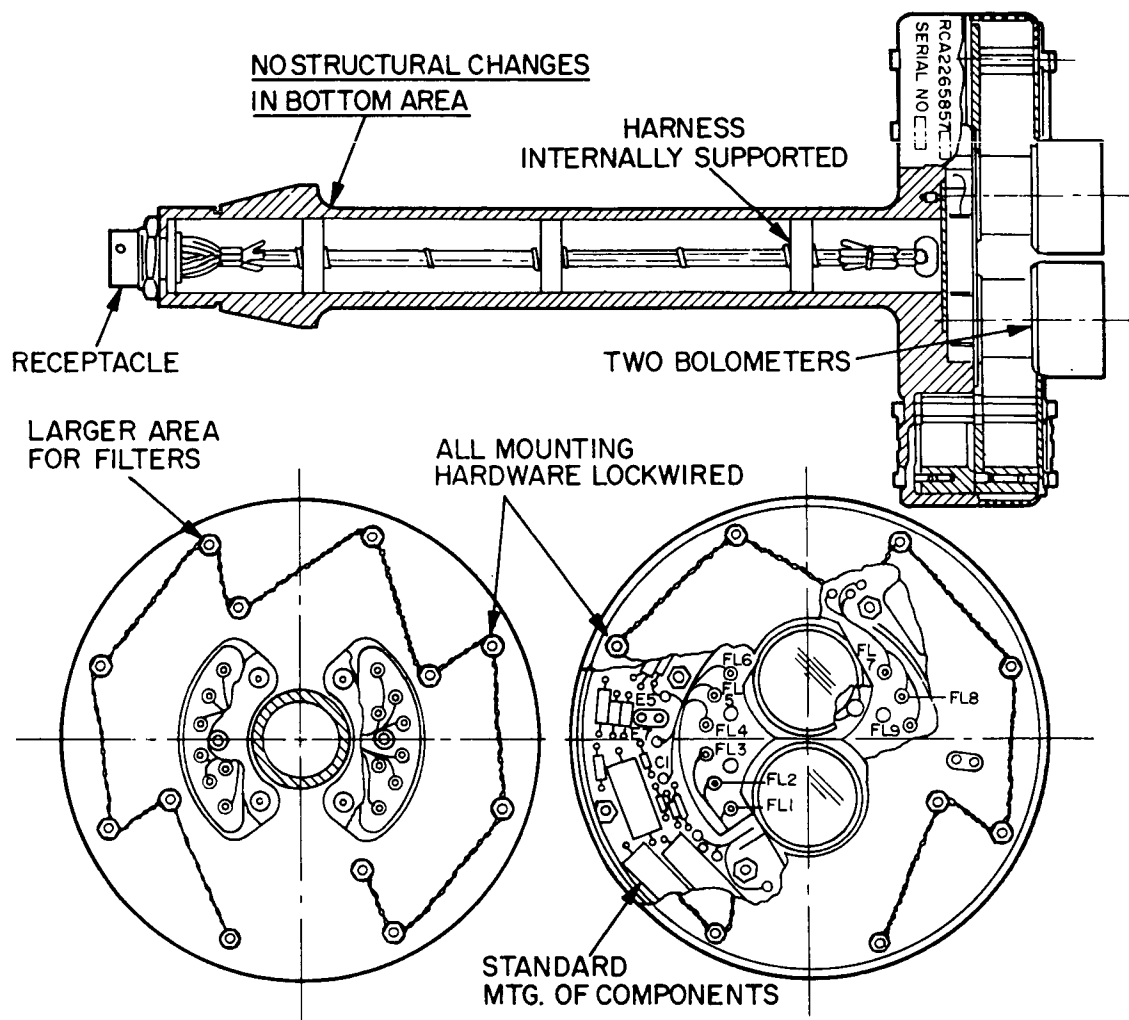


Figure 19. Horizon Sensor Tee Plate

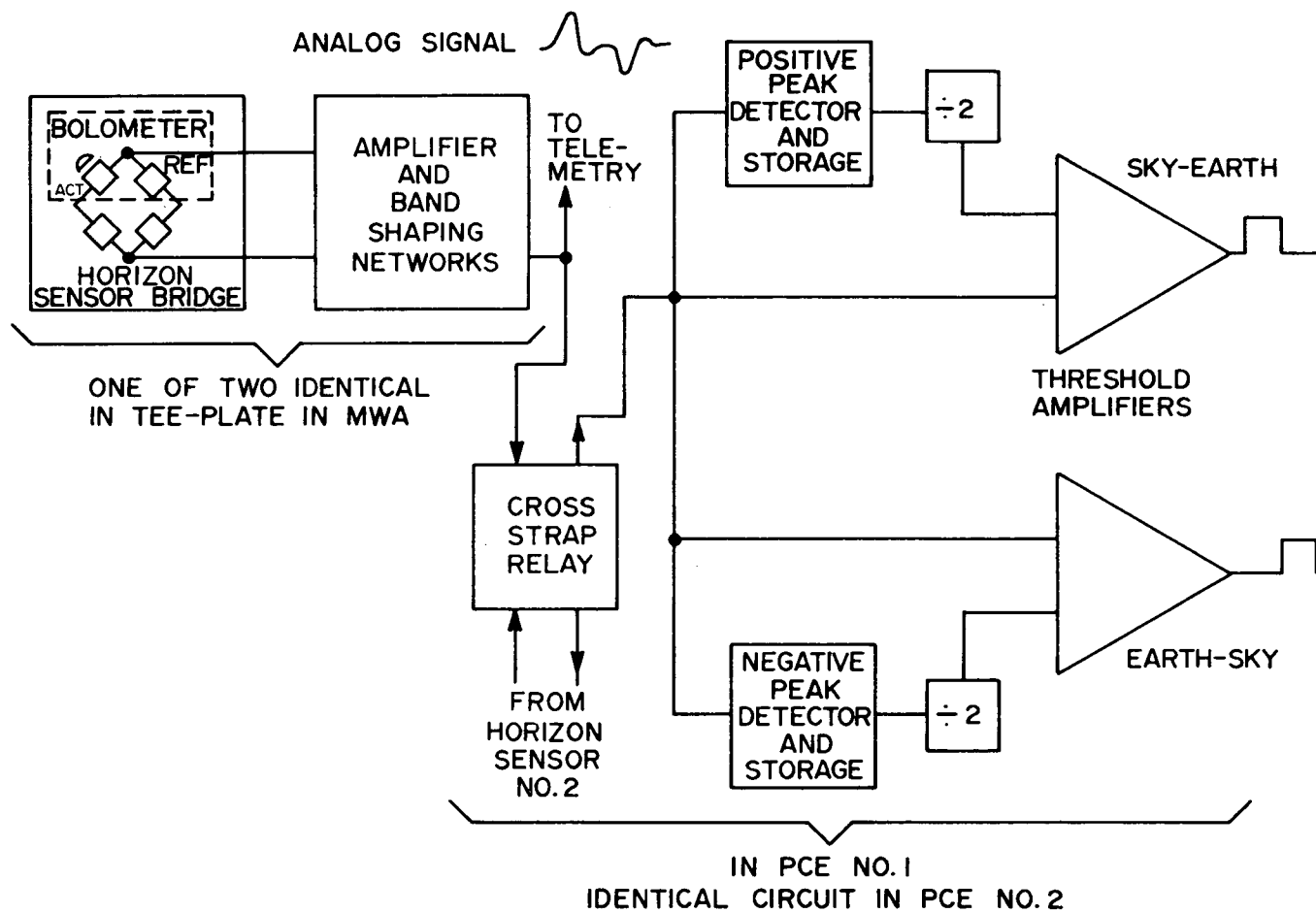


Figure 20. Horizon Sensor, Amplifier and Threshold Circuits

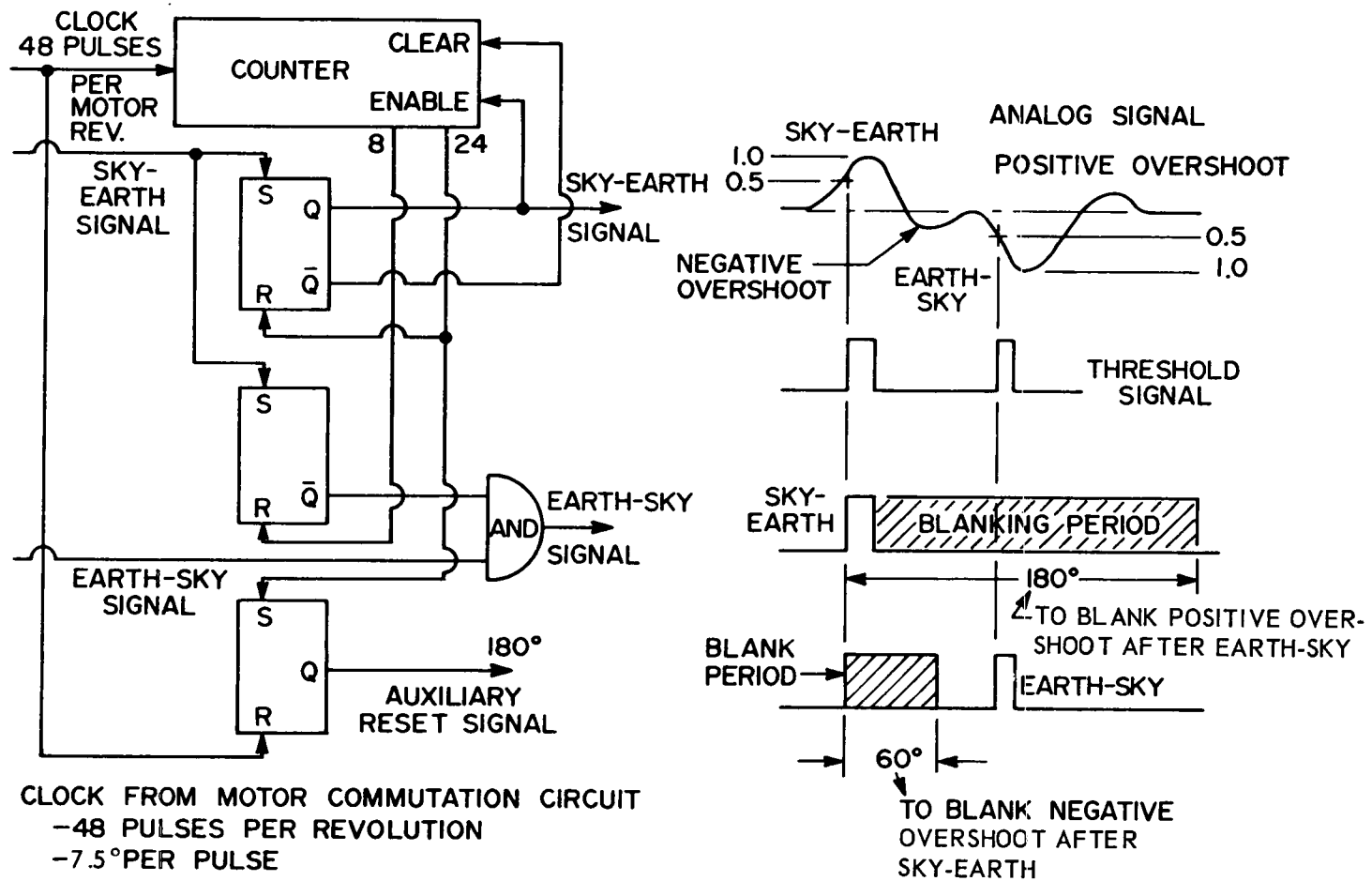


Figure 21. Blanking Circuit

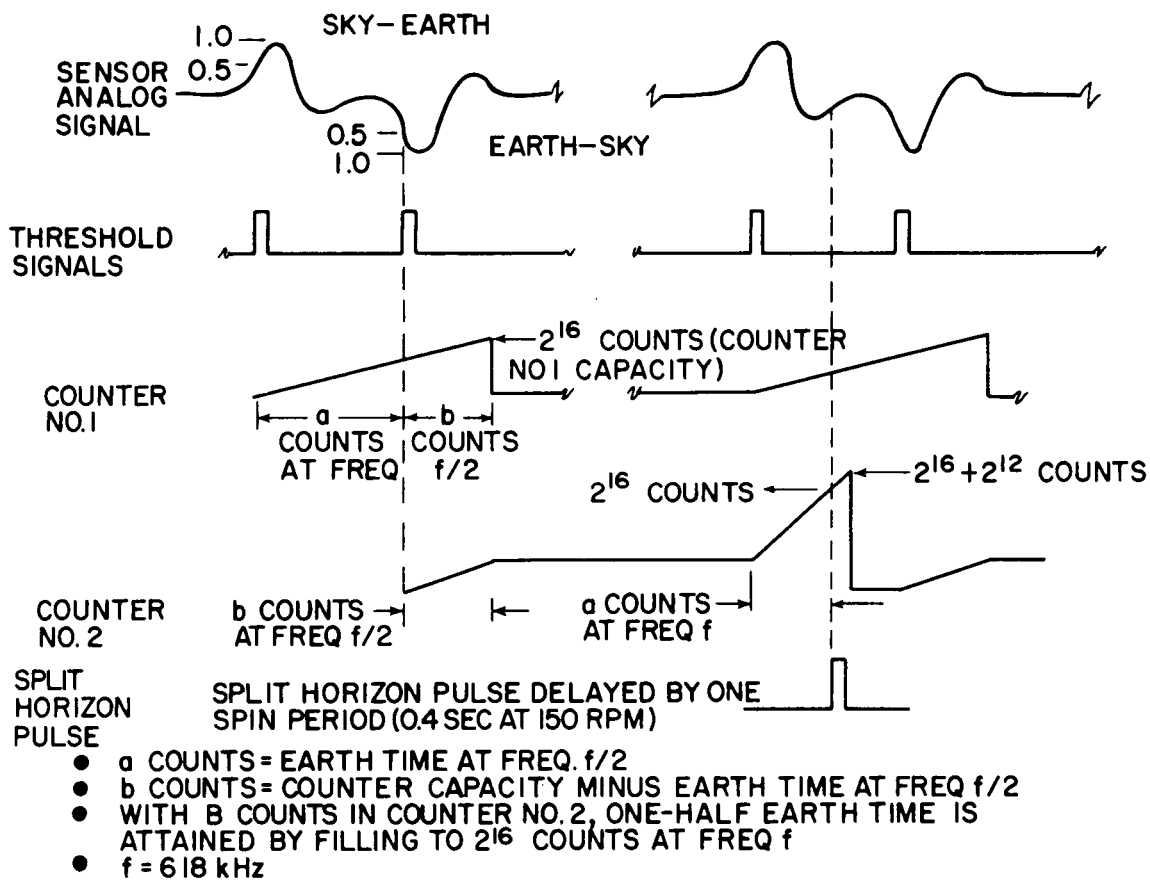


Figure 22. Earth Splitting

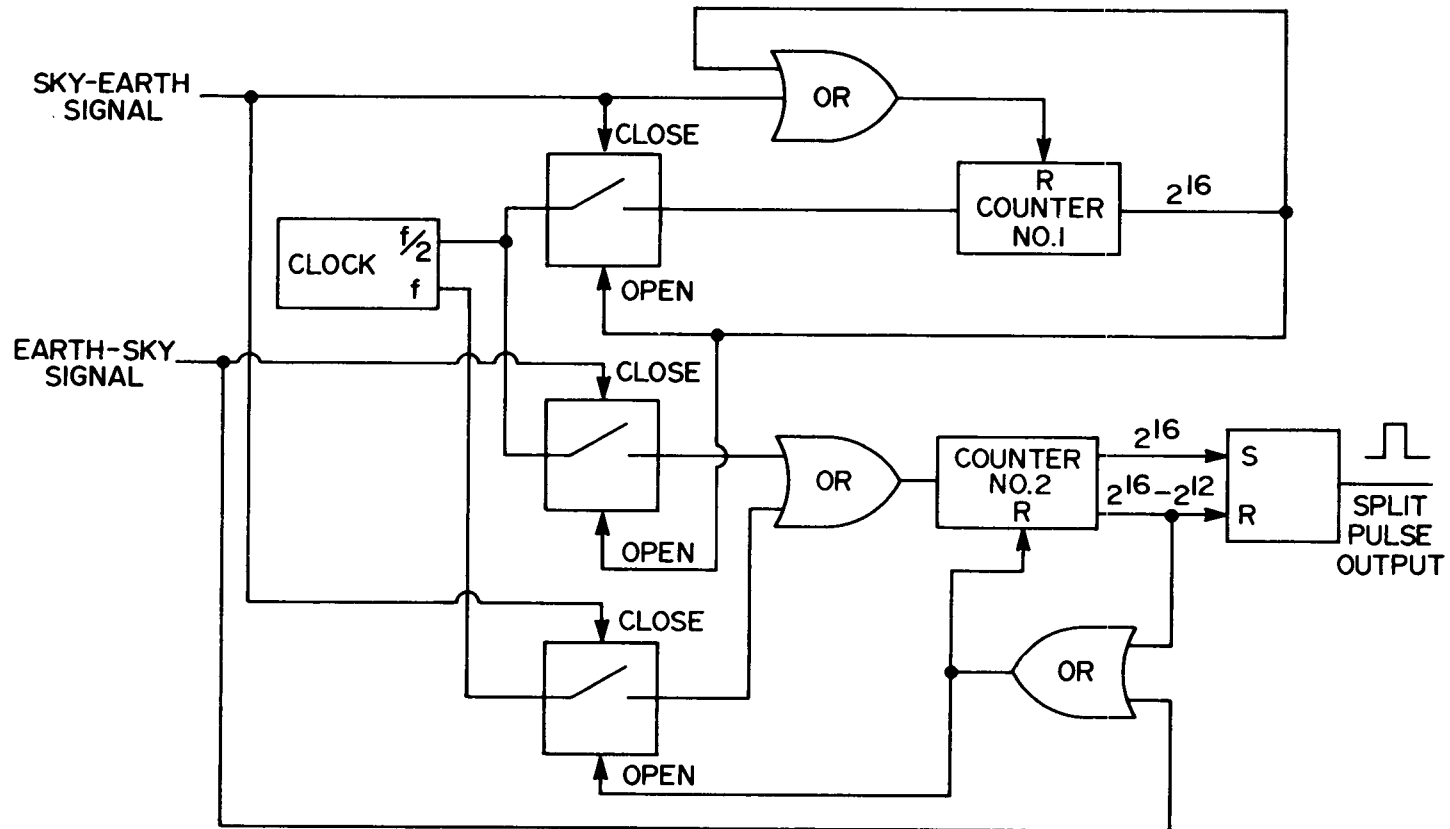


Figure 23. Earth Splitting Circuit

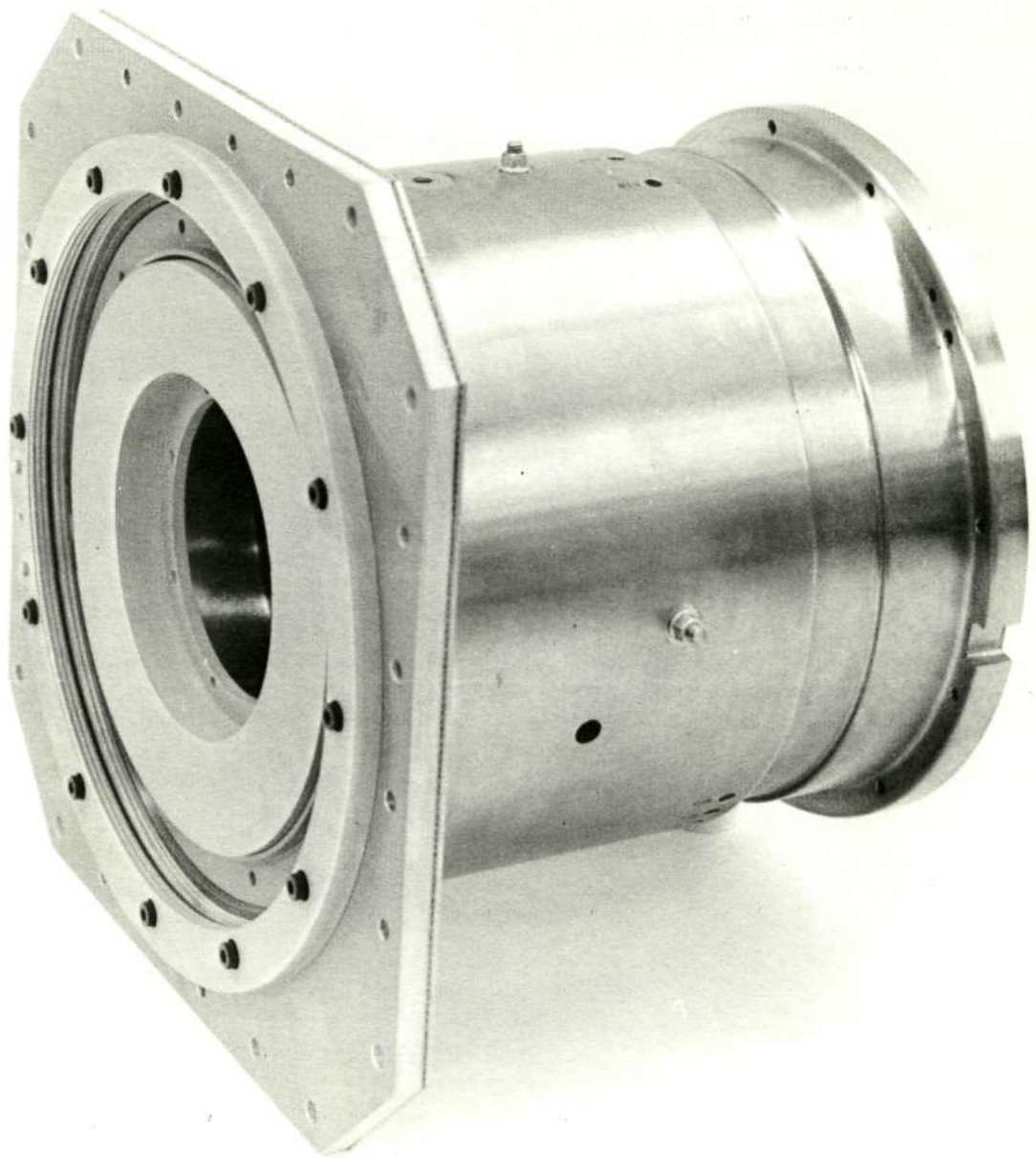


Figure 24. MWA Motor Housing Assembly



Figure 25. MWA Bearing View

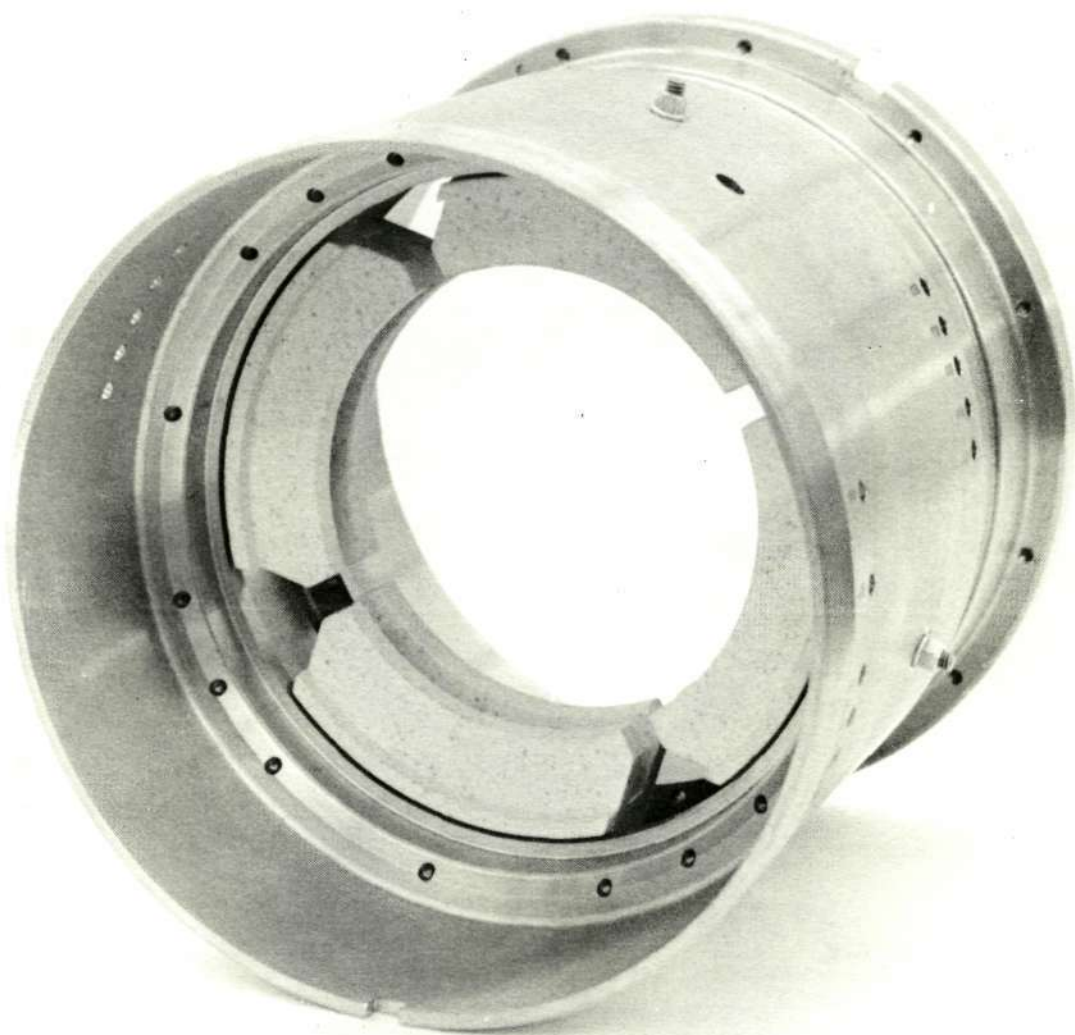


Figure 26. MWA Oil Reservoir View

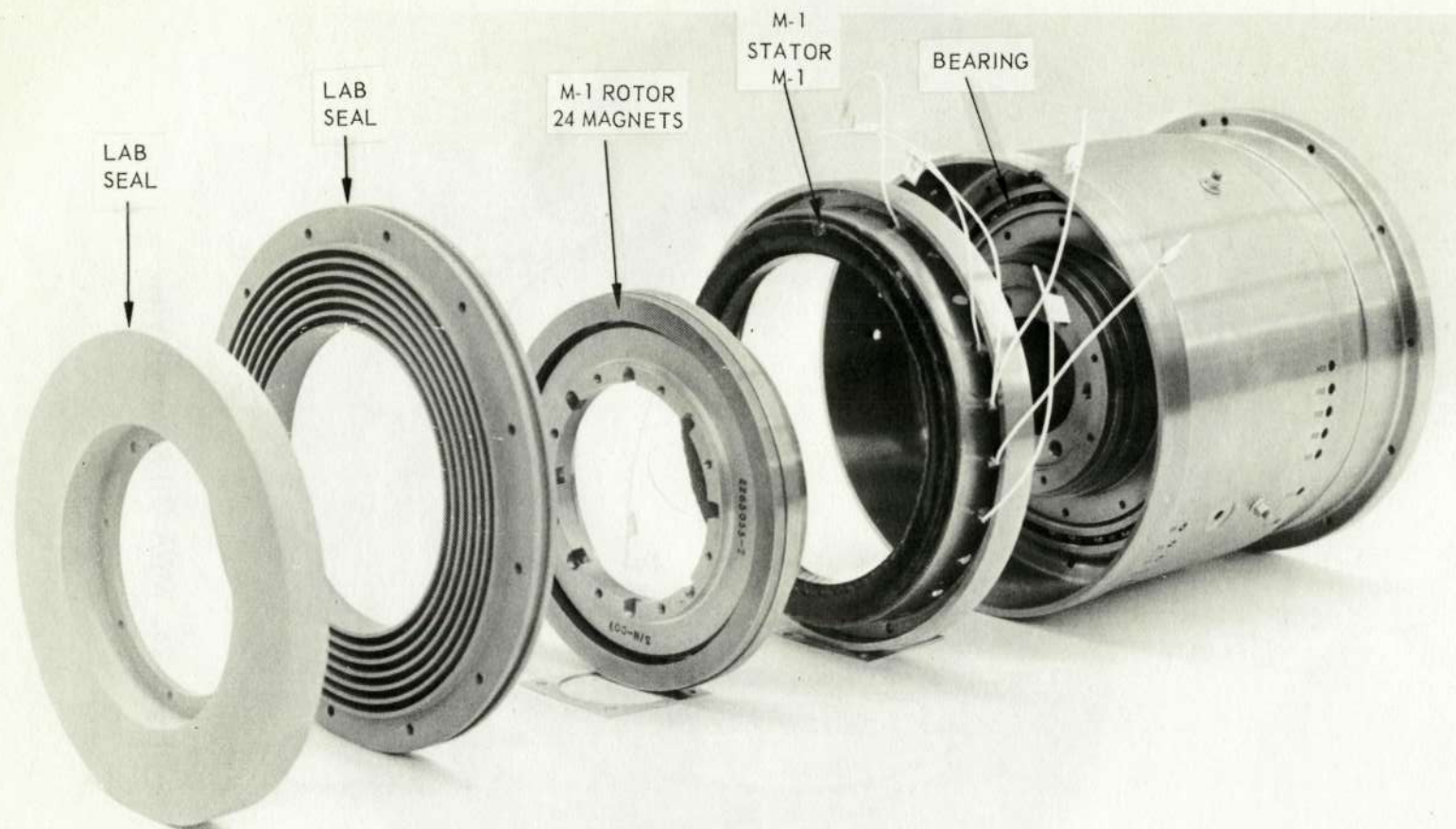


Figure 27. MWA Exploded View – M1 End



Figure 28. MWA Exploded View – M2 End

Reproduced from
best available copy.

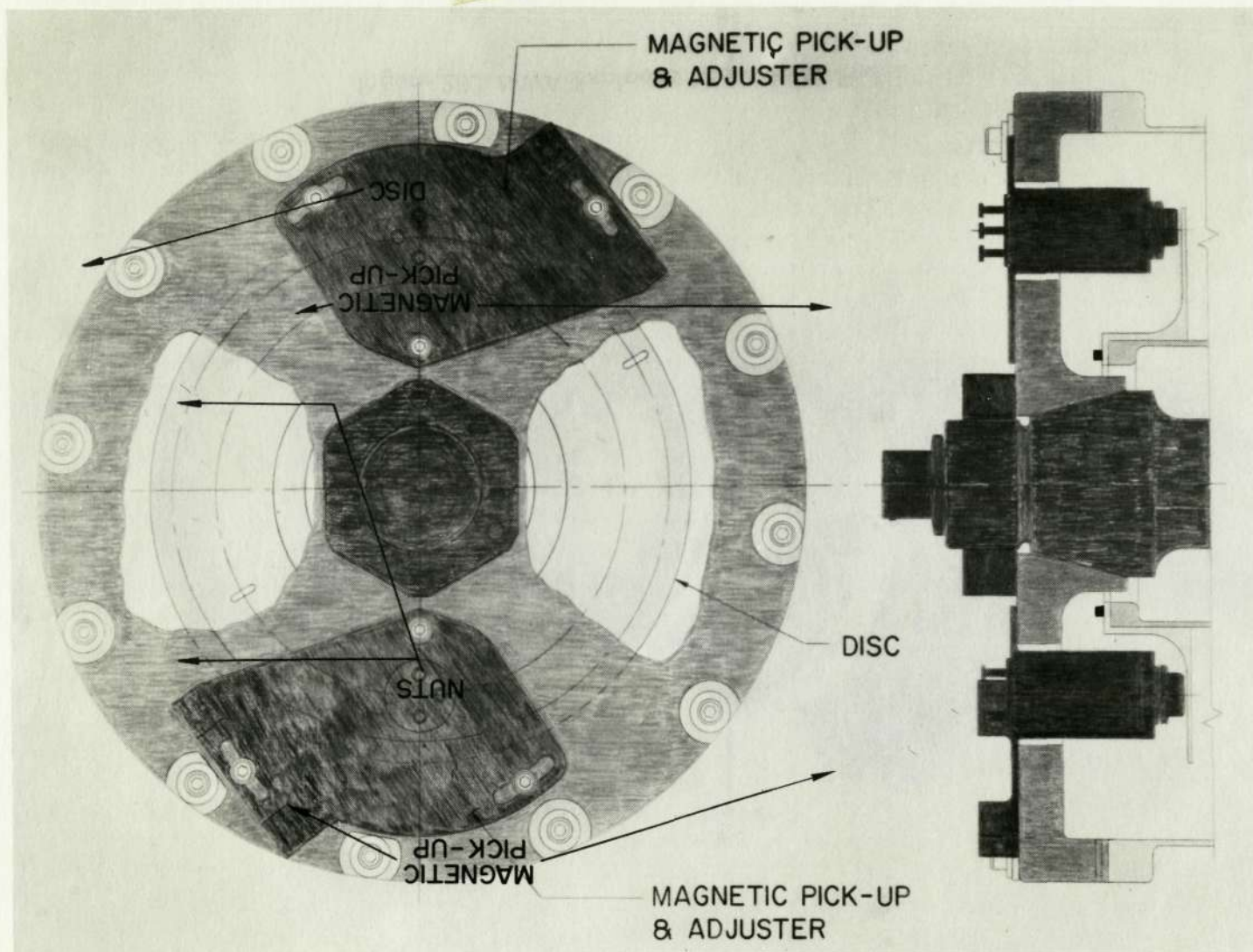


Figure 29. MWA End Cap Cutaway